Shortening the Half-Life of the CRISPR/dCas9 System

Brandon Boodhai Jaunky

A Thesis

In the Department

Of

Biology

Presented in Fulfilment of the Requirements

For the Degree of

Master of Science in Biology at Concordia University

Montreal, Quebec, Canada

September 2023

CONCORDIA UNIVERSITY

School of Graduate Studies

This is to certify that the thesis prepared

By: Brandon Boodhai Jaunky

Entitled: Shortening the Half-Life of the CRISPR/dCas9 System and submitted in partial fulfillment of the requirements for the degree of

Master of Science (Biology)

complies with the regulations of the University and meets the accepted standards with respect to originality and quality.

Signed by the final Examining Committee:

_____ Chair
Dr. Malcom Whiteway

_____ External examiner
Dr. Patrick Gulick

_____ Thesis Co-Supervisor
Dr. William Zerges

_____ Thesis Co-Supervisor
Dr. Nawwaf Kharma

Approved by _____
Dr. Robert Weladji, Graduate Program Director

September 7th, 2023 _____
Dr. Pascale Sicotte, Dean of Faculty

Abstract

Shortening the Half-Life of the CRISPR/dCas9 System

Brandon Boodhai Jaunky, M.Sc.

Shortening the half-life of genetic engineering tools such as dCas9-VP64 can become a pivotal component to regulate many cellular networks, allowing periodic gene expression and protein levels, thereby governing vital cellular processes. However, currently this effector protein has a prolonged half-life in cells and can cause adverse effects by binding to other regions or interacting with other transcriptional or translational machinery. This thesis aims to explore the N-End Rule as a novel approach to achieve shorter half-life dCas9-VP64, offering tighter control for future applications in synthetic circuits.

The need for shorter half-life gene effectors arises from the cytotoxic effects observed with persistence exposure that can lead to off-target effects and unintended modifications, hampering their accuracy and reliability in genetic manipulation. The introduction of short-lived effector proteins also holds significant promise for enhancing temporal control and predictable timing of protein degradation.

The central hypothesis driving this research is that the N-End Rule can be harnessed to shorten the half-life of the artificial transcriptional activator dCas9-VP64 (Varshavsky, 1998). Through site-directed mutagenesis, four amino acids were introduced at the N-terminus of dCas9-VP64, including alanine, valine, serine, and cysteine. These amino acid residues were identified as destabilizing when positioned at N-termini based on the N-acetylation N-End Rule (Nguyen, K.T. et al., 2018).

Experimental design involved genetic construct development, fusion with a fluorescent protein tag for visualization, and validation of N-terminus mutations. Using cycloheximide, a

protein synthesis and translation inhibitor, the steady-state level of the dCas9-VP64-eGFP protein was monitored through eGFP fluorescence from a microplate reader assay and through western blot analysis. We observed different phenotypes during induction and tracking of fusion proteins' signals. Protein half-life was measured using the first order rate kinetic equation for protein degradation.

The results revealed the differential half-life of dCas9-VP64 variants, showcasing the potential of the N-End Rule in achieving shorter half-life. The cysteine variant demonstrated the shortest half-life of 37 minutes, indicating its potential suitability for synthetic circuits. dCas9-VP64-eGFP with the wild-type N-terminus exhibited a half-life of 57 minutes, while serine and alanine variants displayed approximately 54 and 61 minutes, respectively.

In conclusion, this thesis contributes to the advancement of strategies for shortening the half-life of proteins. The implementation of the N-End Rule to achieve this goal exemplifies its potential in optimizing genetic behavior control in future applications with synthetic circuits. By harnessing the N-End Rule, researchers can pave the way for future innovations and advancements in the realm of genetic engineering and molecular biology.

Acknowledgements

I would like to thank my co-supervisors Dr. Nawwaf Kharma and Dr. William Zerges for providing continuous guidance and mentorship for this project, staying patient, and supporting me every step of the way. I want to extend my appreciation to Dr. Malcolm Whiteway who provided critical insight and support for various parts of the project and helped shape many of the experiments.

I would also like to extend my appreciation to my colleagues Devina Singh, Britanny Greco, Joseph Trani who supported me throughout my journey and helped immensely on day-to-day objectives, from Dr. Kachroo's and Dr. Brett's lab.

Furthermore, I would like to thank my brother Dr. Dilan Jaunky who has always been a role model and true source of inspiration for dedicating myself to my career goals and persevering for my objectives.

Most importantly, an immense thank you to my mom and dad for always supporting my decisions and providing all necessary tools and resources to pursue my education.

Table of Contents

LIST OF FIGURES ..... **VII**

LIST OF ABBREVIATIONS ..... **VIII**

SECTION 1: INTRODUCTION **1**

1.1 Brief Overview of CRISPR/dCas9 1
1.2. The Need for Proteins with Shorter Half-Life 3
1.3 Shortening the Half-Life of CRISPR/dCas9-VP64 using the N-end Rule 5
1.4 Thesis Objectives 12

SECTION 2: DIFFERENT N-TERM MUTATIONS VARY IN THEIR FLUORESCENT AND GROWTH KINETICS OF YEAST CELLS EXPRESSING THE FUSION PROTEIN DCAS9-VP64-EGFP **14**

SECTION 3: GALACTOSE-1 PROMOTER INDUCES DCAS9-VP64-EGFP LEVELS BASED ON THE EGFP FLUORESCENCE **25**

SECTION 4: THE CYSTEINE AMINO ACID INSERTION ON THE DCAS9-VP64-EGFP CONSTRUCT FURTHER REDUCES ITS HALF-LIFE. **27**

SECTION 5: DISCUSSION **34**

SECTION 6: MATERIALS AND METHODS **38**

6.1. Strains and Media 38
6.2. Site-Directed Mutagenesis and Gateway Cloning 38
6.3. Fluorescence Micro-plate Reader based Cycloheximide Chase Assay 40
6.4. Live Cell Fluorescence Microscopy 40
6.5. Protein Lysates and Western Blots 41

SECTION 7: REFERENCES **43**

List of Figures

Figure 1. The stabilizing and destabilizing N-term Amino Acids and associated pathways in *S. cerevisiae*

Figure 2. The Gateway Cloning methodology by Yamazaki et al., 1991.

Figure 3. Inducible dCas9-VP64-eGFP fusion construct with different N-term mutations.

Figure 4. Growth Curves of induced and non-induced dCas9-VP64-eGFP variants.

Figure 5. Fluorescent Curves of induced and non-induced dCas9-VP64-eGFP variants.

Figure 6. Growth and fluorescent curves of WT-dCas9-VP64-eGFP.

Figure 7. Growth and fluorescent curves of ALA-dCas9-VP64-eGFP.

Figure 8. Growth and fluorescent curves of VAL-dCas9-VP64-eGFP.

Figure 9. Growth and fluorescent curves of SER-dCas9-VP64-eGFP.

Figure 10. Growth and fluorescent curves of CYS-dCas9-VP64-eGFP.

Figure 11. Fluorescent microscopy of uninduced and induced dCas9-VP64-eGFP variants.

Figure 12. Western blot of full length dCas9-VP64-eGFP variants probed for eGFP during cycloheximide treatment.

Figure 13. Western blot plot intensity analysis of all dCas9-VP64-eGFP variants during cycloheximide treatment.

Figure 14. Western blot plot intensity analysis of eGFP signal from each variant during cycloheximide treatment.

Figure 15. First order rate kinetic curve for protein decay.

Figure 16. Half-Life of dCas9-VP64-eGFP Mutants.

List of Abbreviations

1. UPS - Ubiquitin-Proteasome System
2. N-end Rule - N-end Rule (Principle of protein degradation)
3. gRNA - Guide RNA
4. NATs - N-terminal acetyltransferases
5. CRISPR-Cas9 - Clustered Regularly Interspaced Short Palindromic Repeats and CRISPR-Associated Protein 9
6. dCas9 - Dead Cas9
7. Mxi1 - Max Interactor 1
8. SAM - Synergistic Activation Mediator
9. GFP - Green Fluorescent Protein
10. RFP - Red Fluorescent Protein
11. N-terminus - Amino-terminal end of a protein
12. C-terminus - Carboxy-terminal end of a protein
13. N-acetylation - N-terminal acetylation
14. CRISPRi - CRISPR interference
15. E3 ubiquitin ligases - Ubiquitin ligases that function as enzymes in the ubiquitination process
16. mRNA - Messenger RNA
17. DNA - Deoxyribonucleic Acid
18. RNA - Ribonucleic Acid
19. h - Hours
20. min - Minutes

21. μM - Micromolar

22. NMR - Nuclear Magnetic Resonance

23. DNA-binding domain - Domain of a protein that binds to DNA

24. RNA-binding domain - Domain of a protein that binds to RNA

25. dCas9-VP64 - Dead Cas9 fused with the VP64 transcriptional activator domain

26. α-amino group - Amino group attached to the alpha carbon of an amino acid

27. WT - Wild Type

28. ALA - Alanine

29. VAL - Valine

30. SER - Serine

31. CYS - Cysteine

Section 1: Introduction

1.1 Brief Overview of CRISPR/dCas9

The CRISPR-dCas9, which stands for "Clustered Regularly Interspaced Short Palindromic Repeats - deactivated Cas9," is a revolutionizing gene editing tool that has advanced the field of molecular biology (Tan BC. et al., 2021). Cas9, derived from the bacterial immune system, acts as a molecular scissors that can precisely target and cut specific DNA sequences when combined with a guide RNA that complements the region of interest (Jinek et al., 2012). However, the innovative application of CRISPR-dCas9 goes beyond just DNA cleavage. It lacks the ability to cut DNA, making it a versatile platform for gene regulation. Instead of inducing breaks in the DNA, dCas9 can be guided to specific genomic regions through a customizable RNA molecule (Tan BC. et al., 2021). This technology has enabled highly targeted genetic modifications with applications ranging from basic research to potential therapeutic interventions. The CRISPR-dCas9 system has been further engineered by the fusion to transcriptional activators such the protein complex VP64. The VP64, derived from the herpes simplex virus, functions as a potent activator of gene expression by interacting with transcriptional machinery and enhancing transcription initiation (Omachi et al., 2022). The VP64 domain within the dCas9-VP64 fusion protein plays a pivotal role in enhancing gene expression. It contains multiple repeats of the VP16 activation domain, known for its strong ability to stimulate transcription. Once recruited to the gene's promoter, the VP64 domain interacts with various components of the transcriptional machinery, including transcription factors and co-activators. This interaction leads to the recruitment of RNA polymerase II and initiation of transcription, resulting in increased mRNA production and subsequently elevated protein synthesis (Casas-Mollano JA et al., 2020).

Two problems arise however with this genetic engineering tool, a prolonged half-life which currently is estimated to be above 12 hours and its off-target effects that lead to many toxicities (Shin HY, Wang C et al., 2017). The persistence of dCas9 protein can lead to sustained gene expression even after the initial stimulus has ceased, which is counterproductive for achieving dynamic and controlled gene regulation (Sreekanth V. et al., 2020). To tackle this issue, researchers are exploring innovative strategies to curtail the half-life of CRISPR-dCas9, ensuring a more transient and responsive genetic tool. One of these strategies involves leveraging the N-end rule, a cellular mechanism that governs the stability of proteins based on the identity of their N-terminal amino acids (Varshavsky, 1998, Nguyen, K.T. et al., 2018). By introducing specific destabilizing amino acids at the N-terminus of dCas9, there is a potential strategy at hand to accelerate its degradation and thus achieve a more finely tuned genetic tool. Persistent exposure of this effector protein will have non-specific binding, binding to non-coding regions and binding to other transcriptional machinery for off-target effects. This system holds a lot of potential in editing genomes but is limited to unintended effects due to its long half-life.

These genetic editing tools can also be fused to transcriptional repressors such as the Max Interactor 1 or the Krüppel associated box protein complexes (Gilbert LA. et al., 2013). The inhibition of gene expression can be used to slow or effectively stop pathways that are continuously expressed or mutated to have amplified activity. By combining both protein complexes for transcriptional activation and repression to a genetic engineering tool such as dCas9, these can be further implemented into genetic circuits for oscillatory applications (Kuo J., 2020). The ability to control levels of genetic expression can have potential in restoring natural conditions to dysregulated pathways.

The CRISPR/dCas9 system poses itself as a powerful synthetic biology tool, that through certain modifications such as shortening half-life and fusion to effector proteins, can become a reliable component for synthetic genetic oscillators and have the ability of restoring natural conditions to dysregulated pathways (Charis L Himeda et al., 2016).

1.2. The Need for Proteins with Shorter Half-Life

As the field of synthetic biology advances, researchers seek to engineer proteins with predictable half-life. This property allows the protein to be used in various applications such as short half-life genetic oscillators that maintain functionality (Jonathan Trauth et al., 2019).

A driving factor to identifying strategies to shorten protein half-life is the phenomena of endogenous proteins undergoing mutations and leading to dysregulated pathways (Kondratov et al., 2006). Regulatory proteins that have been mutated to have a prolonged half-life are known to be problematic in organisms. When these regulatory elements have long half-lives, they can persist in the cellular environment for extended periods, even after the original stimuli have subsided. This sustained presence of regulatory elements can lead to continuous gene expression, disrupting the intended temporal dynamics of genetic pathways and causing abnormal behavior. To illustrate, consider the natural gene regulatory network governing circadian rhythms in mammals. The protein complex CLOCK-BMAL1 is a key transcriptional activator that drives the expression of clock genes. In certain mutations of CLOCK-BMAL1, the protein's stability is altered, resulting in a prolonged half-life (Kondratov et al., 2006, Takahashi JS et al., 2008). This extended presence of CLOCK-BMAL1 can disrupt the precise timing of circadian oscillations and lead to detrimental health issues (Kondratov et al., 2006).

Furthermore, the case of the p53 protein provides another example. The p53 protein is a vital regulator of cell cycle and apoptosis (Laptenko et al., 2011). Mutations that extend the half-life of p53 have been associated with increased cancer risk, as the protein's prolonged presence can lead to unchecked cell proliferation and reduced apoptotic responses (Vousden and Prives, 2009). Strategies for shortening the half-life can alleviate these dysregulations.

Developing a genetic engineering tool with a predictable half-life can be utilized to target these mutations and re-establish appropriate genetic expression levels. In contrast to long half-life transcriptional activators or repressors, which can be cytotoxic and perturb normal cellular functions, short half-life genetic effectors minimize these concerns. For instance, the continuous presence of certain transcription factors like Max Interactor 1 in cancer cells could lead to abnormal cell proliferation and malignancy (Eagle LR et al., 1995). Similarly, prolonged expression of tumor suppressor genes like p53 might result in premature cellular senescence, limiting their therapeutic potential (Laptenko et al., 2011). Additionally, the overexpression of certain metabolic enzymes, such as fatty acid synthase, can cause an imbalance in cellular lipid metabolism, contributing to obesity and related disorders (Berndt J. et al., 2007). The need for timed and predictable degradation is further supported by the degradation of the transcription factor Sterol regulatory element-binding protein 1 that needs to be within hours to prevent the excessive accumulation of lipids thereby maintaining metabolic homeostasis (Ponugoti B. et al., 2010). With regards to cell division, the transient expression of cell cycle regulators like Cyclin B prevents inappropriate cell division, ensuring genome stability (Clute and Pines, 1999). These examples support the need for strategies to shorten the half-life of proteins, re-establish genetic expression levels by reliable genetic engineering tools such as dCas9-VP64.

1.3 Shortening the Half-Life of CRISPR/dCas9-VP64 using the N-end Rule

Reducing the half-life of dCas9 provides several benefits for fine-tuning the CRISPR/Cas9 system. Enhanced temporal control over Cas9 activity can minimize the risk of off-target effects and ensure more specific and controlled gene regulation, as previously mentioned (Sreekanth V. et al., 2020). Researchers have then employed several strategies to shorten the half-life of the CRISPR/dCas9 system. In some cases, by introducing destabilizing domains to dCas9, an accelerated turnover of dCas9 activity was achieved (Balboa D. et al., 2015). Previous strategies to regulate dCas9 activity have included the use of Proteolysis Targeting Chimeras and cyclins. Proteolysis Targeting Chimeras are small molecules designed to recruit specific E3 ligases to target proteins for ubiquitination and degradation (Neklesa et al., 2017). From which a new category emerged named, Transcription Factor Targeting Chimeras, which uses a chimeric oligonucleotide to bind to the transcription factor activator such as dCas9-VP64 (Samarasinghe KTG. et al., 2021) However, the effectiveness of these can be influenced by the cellular context and the availability of E3 ligases. In one study using Proteolysis Targeting Chimeras to degrade dCas9, it was reported that dCas9 degradation took more than 24 hours after the treatment (Neklesa et al., 2017, Samarasinghe KTG. et al., 2021). This slow degradation rate limits the precision of temporal control required. Another approach involves utilizing destabilization domains attached to the N-termini of proteins. Specifically, the "DD" (Degradation Domain) system, which employs a unique approach to enhance temporal control over dCas9 activity. The dCas9 system was attached to a protein of 12 kDa, originating from a peptidyl isomerase family of proteins and where in the presence of a small molecule called Shield-1, the dCas9 remains stable. Upon removal of Shield-1, the DD destabilizing domain initiates degradation of dCas9 (Senturk S. et al., 2017). This synthetic domain is strategically incorporated into the dCas9 protein, rendering it highly

susceptible to degradation. Despite the potential of shortening dCas9 half-life to create oscillating genetic circuits, there are critical optimization challenges that require attention. The choice of destabilizing domains and their effectiveness in accelerating protein degradation still requires optimization to achieve half-life of minutes.

The N-end rule, discovered by Alexander Varshavsky, dictates that the N-terminal amino acid of a protein can influence its stability and its susceptibility to degradation. This can potentially be a strategy employed to shorten the half-life of dCas9-VP64 (Nguyen KT et l., 2019, Naumann C. et al., 2016). Under this rule, several pathways exist such as the N-end acetylation rule that prepares proteins for degradation (**Figure 1)**. The N-end acetylation rule, with its covalent attachment of an acetyl group to the α-amino group of the N-terminal amino acid of a protein, exhibits remarkable conservation across eukaryotic organisms, indicating its fundamental significance in cellular processes (Nguyen, K.T. et al., 2018, Aksnes et al., 2016, Varshavsky, 1998). This conserved mechanism spans from yeast to humans and constitutes a crucial modification affecting numerous cellular events. Notably, proteins harboring methionine, serine, alanine, glycine, threonine, cysteine, or valine at their N-terminus are more likely to undergo N-terminal acetylation, leading to distinct functional consequences (Polevoda & Sherman, 2003).

The major pathway for intracellular protein degradation related to the N-end Rule is the Ubiquitin Proteasome System pathway. The UPS involves a series of enzymatic reactions mediated by three types of enzymes: E1 ubiquitin-activating enzymes, E2 ubiquitin-conjugating enzymes, and E3 ubiquitin ligases. The E1 enzyme activates ubiquitin and forms a thioester bond between the C-terminal glycine of ubiquitin and a cysteine residue in the E1 enzyme (Hershko & Ciechanover, 1998, Tanaka K., 2013). Once activated, ubiquitin is transferred to an E2 enzyme through a trans-thioesterification reaction. In the context of N-terminal acetylated proteins, the

next step involves the recruitment of a specific E3 ubiquitin ligase that recognizes the acetylated N-terminus as a degron. One such E3 ligase is Ubr1, a well-known E3 ligase in yeast (Swanson et al., 2001, Khosrow-Khavar F., et al. 2016). Ubr1 binds to its substrate proteins, recognizing N-terminal degrons such as acetylated serine or alanine residues (Khosrow-Khavar F., et al. 2016). Upon substrate recognition, Ubr1 catalyzes the covalent attachment of ubiquitin to the substrate protein's N-terminal acetyl group, marking it for degradation. This process involves the formation of an isopeptide bond between the C-terminal glycine of ubiquitin and the ε-amino group of a lysine residue on the substrate protein. The resulting polyubiquitinated protein is now targeted for proteasomal degradation (Swanson et al., 2001, Khosrow-Khavar F., et al. 2016).

Following recognition, the 19S regulatory particle of the proteasome unfolds the polyubiquitinated protein, preparing it for degradation within the central chamber of the 20S core particle. This unfolding process requires ATP hydrolysis and is facilitated by ATPase subunits within the proteasome complex (Bard JAM. et al., 2005, Tanaka K., 2013). The unfolding of the substrate protein exposes its peptide bonds, making it accessible for proteolytic cleavage.

The proteolytic degradation occurs within the proteasome's core particle, also known as the 20S proteasome, where the active sites for protein cleavage reside. The 20S proteasome is a cylindrical structure formed by four stacked rings, each containing seven subunits (Bard JAM. et al., 2005, Groll et al., 1997). Once inside the 20S proteasome, the polyubiquitinated protein undergoes proteolytic cleavage, resulting in the generation of small peptide fragments typically 7-9 amino acids in length (Pickart & Cohen, 2004). These peptide fragments are then released from the proteasome and further degraded by cytosolic peptidases, eventually recycled into amino acids that can be utilized for new protein synthesis or other cellular processes (Goldberg, 2003). These active sites of the 20S proteasome include caspase-like, trypsin-like, and chymotrypsin-like

activities, which exhibit different substrate specificities and cleavage preferences (Groll et al., 1997). The sequential action of these proteolytic sites ensures the complete degradation of the polyubiquitinated protein into short peptides.

The proteasome's ability to degrade polyubiquitinated proteins is essential for maintaining protein homeostasis and cellular function. It regulates the levels of key regulatory proteins, mediates the turnover of damaged or misfolded proteins, and controls the abundance of various cell cycle regulators and signaling molecules (Hershko & Ciechanover, 1998).

Stabilizing N-Terminal Amino Acids	**Destabilizing N-Terminal Amino Acids**	**Applicable N-End Rule Pathway**
Arginine (Arg, R)	Aspartate (Asp, D)	N-Arginylation
Lysine (Lys, K)	Valine (Val, V))	N-Acetylation
Leucine (Leu, L)	Asparagine (Asn, N)	N-Arginylation
Phenylalanine (Phe, F)	Glutamine (Gln, Q)	N-Arginylation
Tryptophan (Trp, W)	Serine (Ser, S)	N-Acetylation
	Threonine (Thr, T)	N-Arginylation
	Cysteine (Cys, C)	N-Acetylation
	Glycine (Gly, G)	N-Arginylation
	Alanine (Ala, A)	N-Acetylation

Figure 1. The stabilizing and destabilizing N-Term Amino Acids and associated Pathway in *S. cerevisiae.* The amino acids based on the N-end rule is associated with a conserved pathway found in eukaryotes, where it is either considered stabilizing or destabilizing based on the covalent attachments of an acetyl group or arginine amino acid to the n-term of the protein.

The N-end acetylation rule is a well-established and conserved pathway that is linked to triggering the ubiquitin-proteasome system (UPS) for protein degradation in various eukaryotic organisms, including yeast (Aksnes et al., 2016). N-terminal acetylation is one of the most prevalent protein modifications in eukaryotic cells, with an estimated 80% of all human proteins being N-terminally acetylated (Arnesen et al., 2009). Specifically, proteins with certain amino acids, such as serine (S), alanine (A), cysteine (C), or valine (V), at their N-terminus are more prone to acetylation than those with other amino acids.

This acetylation is completed by a group of enzymes conserved in yeast. Yeast contains five different N-term Acetyltransferases (NATs): NatA, NatB, NatC, NatD, and NatE, each with specific substrate specificity (Starheim et al., 2009, Starheim et al., 2012). Researchers identified that the NatA complex is an important key enzyme in yeast cell growth and protein stability (Deng & Marmorstein, 2021). This intricate complex is composed of two subunits, Ard1 and Nat1. Notably, the subunit Ard1, initially named "Arrest-Defective 1," gained its distinctive nomenclature from its intriguing role in cell cycle progression and its linkage to cell cycle arrest phenotypes (Kuo HP & Hung MC, 2010). Expanding the understanding of the Nat complexes, Starheim et al. (2009) contributed to the field by investigating NatB, revealing its substrate specificity for N-terminal methionine and specific amino acids positioned adjacent to it (Starheim et al., 2009). This meticulous analysis shed light on sequence preferences that govern the acetylation process carried out by NatB. The family of N-terminal acetyltransferases continues with the NatC complex. Polevoda and Sherman's work in 2001 provided insights into NatC's role in acetylating proteins with N-terminal serine or alanine (Polevoda & Sherman, 2001). This discovery added depth to our understanding of substrate specificity among the Nat complexes.

NatC, composed of subunits Mak3, Mak10, and Mak31, is involved in maintaining protein stability and influencing cellular processes (Polevoda & Sherman, 2001).

Further exploration led to the characterization of NatD and NatE complexes, with Aksnes and his colleagues dissecting their distinct substrate specificities, guided by specific sequence motifs (Aksnes et al., 2015). These studies highlighted the complexity and diversity within the NAT network. NatD, consisting of Naa30 and Naa35 subunits, acetylates proteins with a methionine or glycine and finally, NatE, composed of Naa40 and Naa45 subunits. (Van Damme P. et al., 2015).

After these NATs catalyzes the transfer of an acetyl group to the N-terminal serine (S), alanine (A), cysteine (C), or valine (V) of a substrate protein, the acetylated protein can undergo further processing and trafficking, ultimately influencing its fate within the cell. In some cases, N-terminal acetylation serves as a signal for targeting specific proteins to the ubiquitin-proteasome system (UPS). As this system it most likely determines the half-life of dCas9, increasing the recognition of this protein for ubiquitination and proteasomal degradation will likely decrease this half-life. The N-terminal amino acid residue is a key determinant in the rate of poly-ubiquitination of a protein and, hence, controlling the half-life of dCas9.

In summary, incorporating the N-end rule into the design of the dCas9-VP64 construct, we aim to shorten its half-life, enabling precise temporal control over gene expression. This strategy involves introducing specific destabilizing N-terminal amino acids, such as alanine, valine, serine, or cysteine, based on their characterizations as N-end rule destabilizing residues (Tasaki et al., 2012).

1.4 Thesis Objectives

The objective of this MSc project is to investigate the N-end rule as a strategy for effectively achieving shorter half-lives of gene effectors, specifically focusing on the transcriptional activator dCas9-VP64. The significance of shorter half-lives lies in the potential to create a more precise and tightly regulated tool for gene editing and manipulation of key pathways. Current studies have highlighted the cytotoxic effects associated with prolonged exposure to dCas9 and its variants, emphasizing the need for better temporal control.

The main hypothesis driving this research is that the N-end rule pathway, specifically the N-acetylation N-end rule, can serve as a method to shorten the half-life of dCas9-VP64. To test this hypothesis, site-directed mutagenesis was employed to introduce four destabilizing amino acids (alanine, valine, serine, and cysteine) at the N-terminus of dCas9-VP64. Previous literature has characterized these specific amino acids as having destabilizing N-termini due to their high susceptibility to N-terminal acetyltransferases, which subsequently triggers the N-end rule pathway.

Chapter 2 of this thesis will provide a comprehensive description of the experimental design and rationale behind the genetic constructs. The approach required adherence to specific criteria for proper characterization. Moreover, the choice of the cloning method, specifically the utilization of the Gateway cloning method, allowed successful fusion of dCas9-VP64 to the fluorescent protein tag eGFP on the C-terminus. This fusion protein was regulated by the galactose-inducible promoter GAL1, enabling inducible expression for tracking purposes. The constructs were subjected to verification, and the sequencing analysis confirmed the successful mutation of the N-termini of each variant. In the subsequent sections of Chapter 2, the results from microplate fluorescence reader assays will be presented. The experiments were conducted with

and without the addition of cycloheximide, a protein synthesis inhibitor, that allowed to track the steady-state level of the eGFP fluorescent signal. These assays allowed for the observation of different phenotypes during induction and tracking of the fusion protein signal.

Chapter 3 showcases the visual confirmation of cells expressing the genetic constructs and the fusion protein under different conditions using fluorescent microscopy. This visualization offers valuable evidence for the inducible expression of dCas9-VP64-eGFP driven by the GAL1 promoter, further validating the function of the nuclear localization signal in the sequence.

Finally, in Chapter 4, a detailed description of the cycloheximide chase assay will be provided. This assay played a crucial role in revealing the changes in half-life for each N-term variant of dCas9-VP64. Protein quantification with western blotting allowed for the quantification and comparison of protein decay rates among the different variants. Notably, the cysteine variant exhibited a significantly shorter half-life compared to the other variants, highlighting the potential influence of this specific N-terminal amino acid on the degradation dynamics.

Looking ahead, future directions for this research involve exploring additional strategies for achieving shorter half-lives of gene effectors. One avenue is to investigate the possibility of incorporating tandem cysteine units to enhance the destabilizing effect. Additionally, exploring other N-terminal amino acids with destabilizing properties may further contribute to refining the temporal control of dCas9-VP64. Moreover, inhibiting the proteasome and tracking degradation of dCas9-VP64 further reveal if the UPS pathway is responsible for its turnover. Ultimately, these advancements will enhance the field of genetic engineering tools and the predictability in protein half-lives.

Section 2: Different N-Term Mutations Vary in their Fluorescent and Growth Kinetics of Yeast Cells Expressing the Fusion Protein dCas9-VP64-eGFP.

The yeast codon optimized dCas9-VP64 was the protein of interest that was studied through destabilization of its N-terminal via site-directed mutagenesis. It would be expected that mutations in the N-terminal would cause the protein to become targeted for degradation allowing a faster protein turnover. The aim of this experiment is to build four constructs of dCas9-VP64-eGFP containing different mutations at their N-terminal to indirectly study stability of the protein using the green fluorescent protein signal.

The experimental design involved monitoring the start and stop of the protein synthesis and the effects of the N-terminal mutations on each of their kinetic profiles. This was accomplished using Gateway cloning (**Figure 2**) to fuse ALA-dCas9-VP64, VAL-dCas9-VP64, SER-dCas9-VP64, and CYS-dCas9-VP64 to eGFP on each of their C-termini while under regulatory control of the galactose inducible promoter GAL1. Using the Gateway cloning method (**Figure 2**), the dCas9-VP64 gene was successfully integrated in to the pDONR221 vector with the attB overhangs, preparing it for the final LR reaction in to the pAG416-ccdb-eGFP destination vector.

Gateway cloning of the designed constructs in **Figure 3A** were successfully assembled as confirmed by sequence verification (**Figure 3B**). Through sequence verification we were also able to verify that no frameshift was present after insertion of the codon in the sequences which could skew the end-results. Additionally, a nucleotide sequence alignment search was done using NCBI BLAST to confirm that each construct maintained the wild-type dCas9-VP64 sequence with 99.92% similarity.

Sequencing results also showed the expected base pair numbers of 10,472 bp for dCas9-VP64 (WT) and 10,475 base pairs for each other point-mutated constructs (ALA, CYS, VAL, and

SER). Successful isolation of *S. cerevisiae* BY4741 colonies containing fully assembled and sequence verified dCas9-VP64-eGFP, ALA-dCas9-VP64-eGFP, VAL-dCas9-VP64-eGFP, SER-dCas9-VP64-eGFP, CYS-dCas9-VP64-eGFP were obtained.

Expression of each construct using the inducible *GAL1* promoter was tested with 2% glucose and eGFP fluorescent signal was measured using a microplate reader (**Figure 5A**). We observed that a 2% glucose induction over 24 hours achieved a maximal fluorescence intensity of approximately 28,000 A.U., for all N-terminal variants including wildtype (**Figure 5A**). All variants revealed a sigmoidal curve and reached their maxima after 12 hours of induction. In contrast, when they were induced with 2% galactose (**Figure 5B**), each variant achieved higher fluorescence maxima, except VAL-dCas9-VP64-eGFP mutant, which was comparable to 2% glucose induction. The fluorescent maxima for dCas9-VP64-eGFP, ALA-dCas9-VP64-eGFP, VAL-dCas9-VP64-eGFP, SER-dCas9-VP64-eGFP, CYS-dCas9-VP64-eGFP was 137,000 A.U., 84,000 A.U., 25,000 A.U., 149,000 A.U., and 220,000 A.U., respectively. We noticed that CYS-dCas9-VP64-eGFP mutant had a 1.6-fold higher fluorescence intensity compared to dCas9-VP64-eGFP. We also monitored the growth of each variant using optical density, to verify any changes in growth parameters. We noticed that the stationary phase in 2% glucose induction was achieved at approximately 12 hours whereas 2% galactose induction was achieved at approximately 18 hours. The growth curve was used to determine the mid-log point where cycloheximide treatment was added to halt protein synthesis and measure protein kinetics through change in fluorescence. At time point 5 hours was the mid log point selected for the following assays.

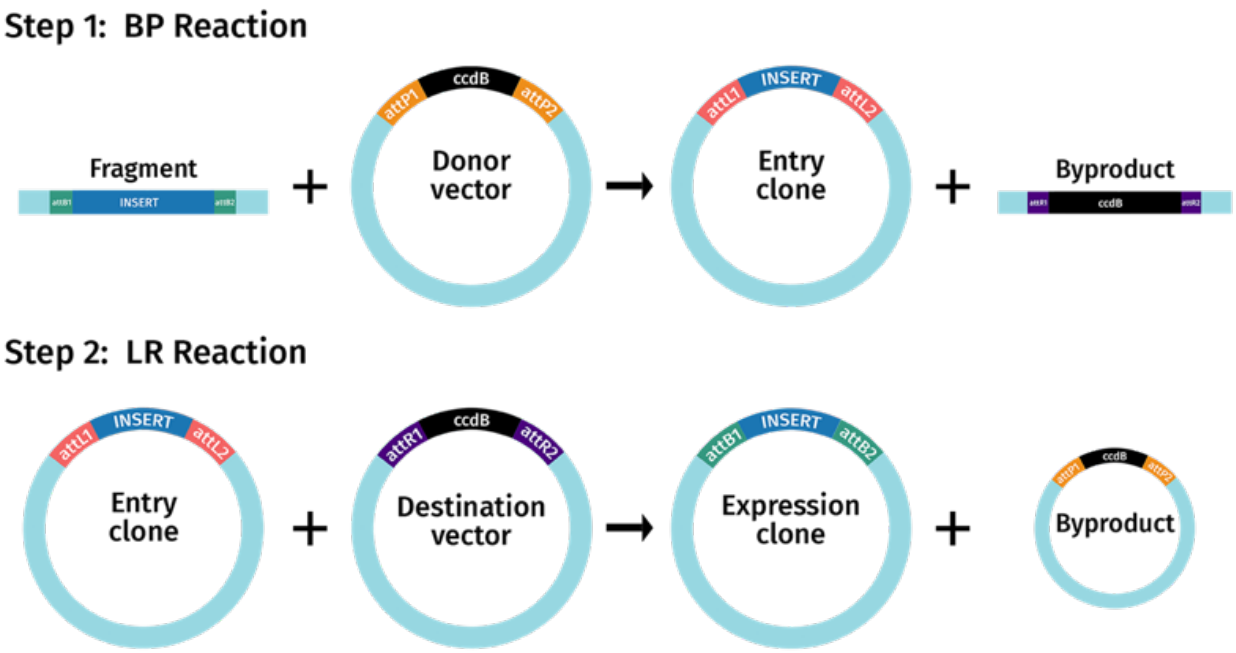

Figure 2. Gateway cloning methodology by Yamazaki et al., 1991. (Snapgene). The Gateway Cloning method utilizes two vectors where the flanking regions of homology allow inserts to swap into subsequent destination vectors in the presence of clonases.

A

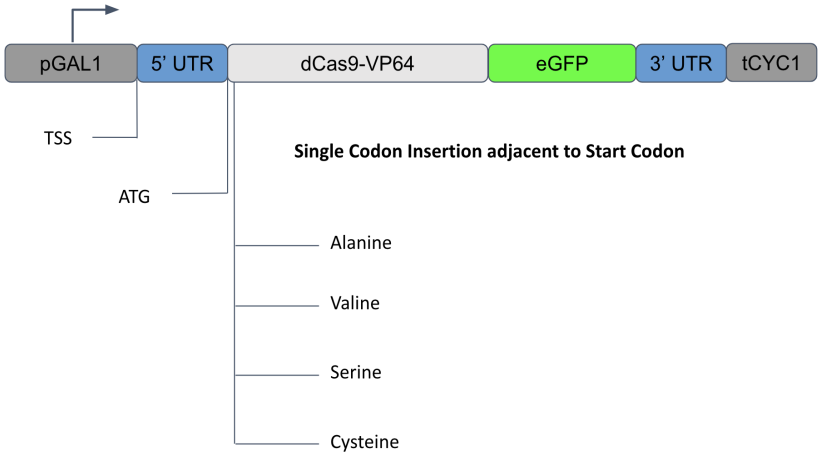

B

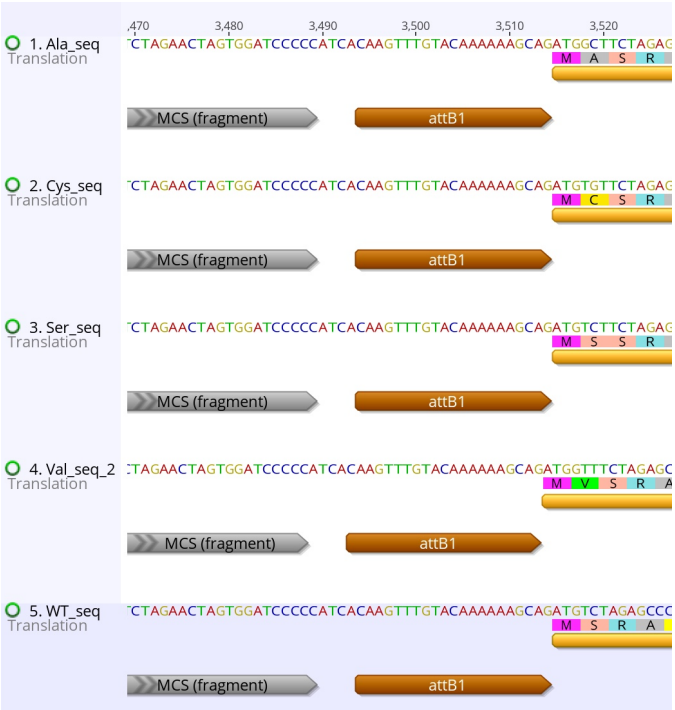

Figure 3. Inducible dCas9-VP64-eGFP fusion construct with different N-term mutations. A. The genetic construct of dCas9-VP64 with a galactose-1 promoter and fused to the eGFP at the c-term. The different n-terms are directly adjacent to the methionine amino acid**. B.** Sequence verification to confirm insertion of each amino acid.

A

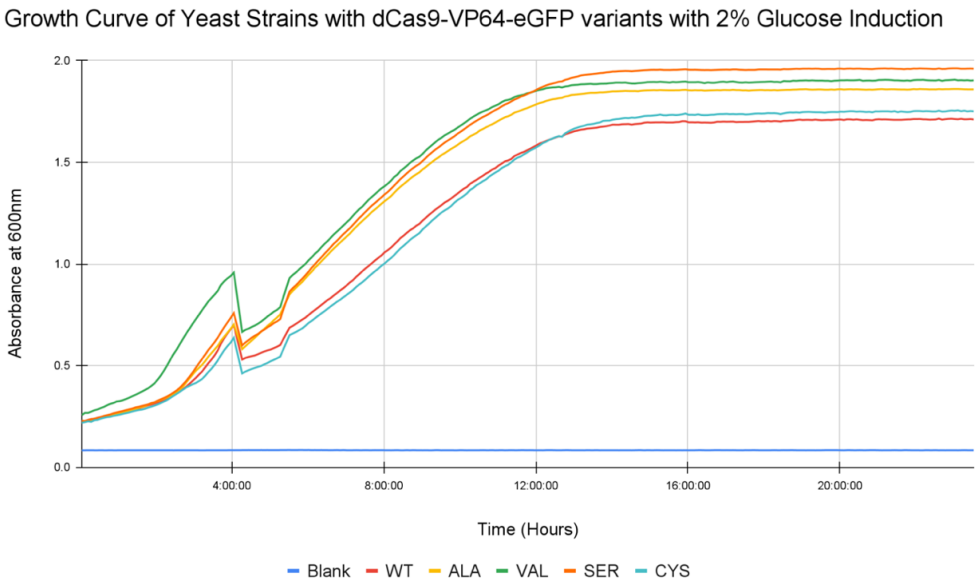

B

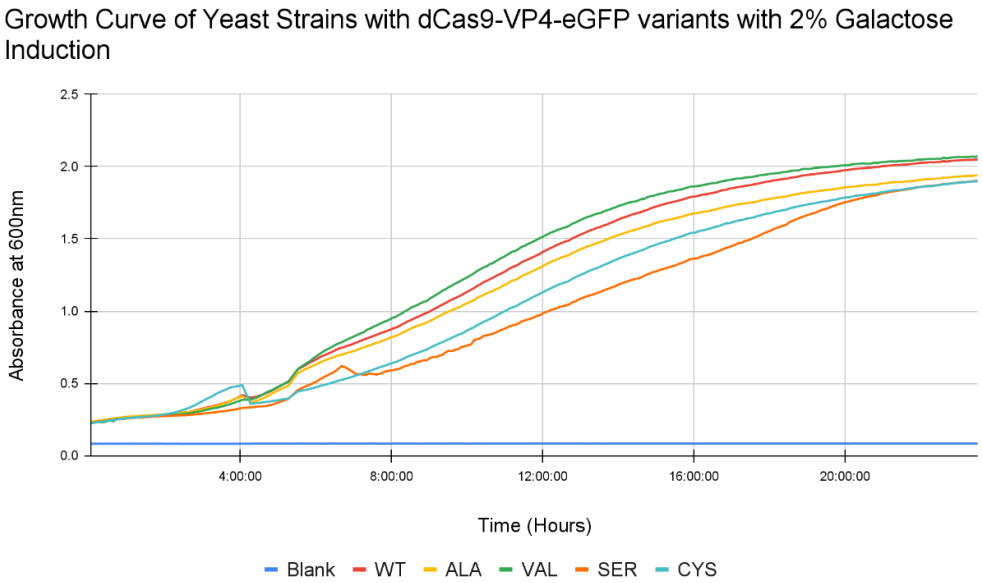

Figure 4. Growth Curves of induced and non-induced dCas9-VP64-eGFP variants. A. All yeast transformants grown with 2% glucose, no cycloheximide, over 24 hours recorded optical density at 600 nm. **B.** All yeast transformants grown with 2% galactose, no cycloheximide, over 24 hours, recorded optical density at 600 nm.

A

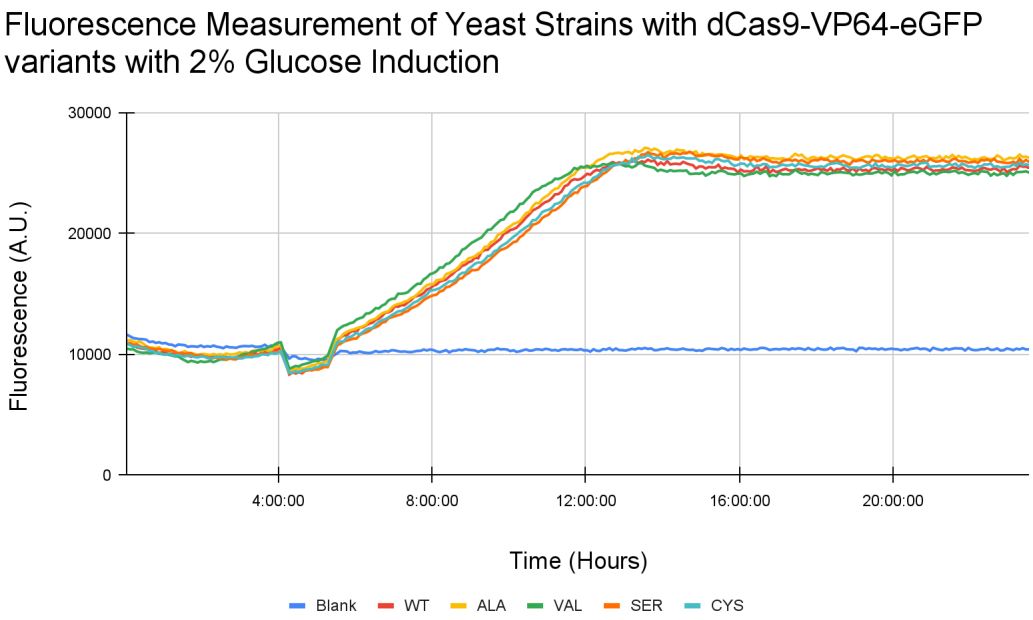

B

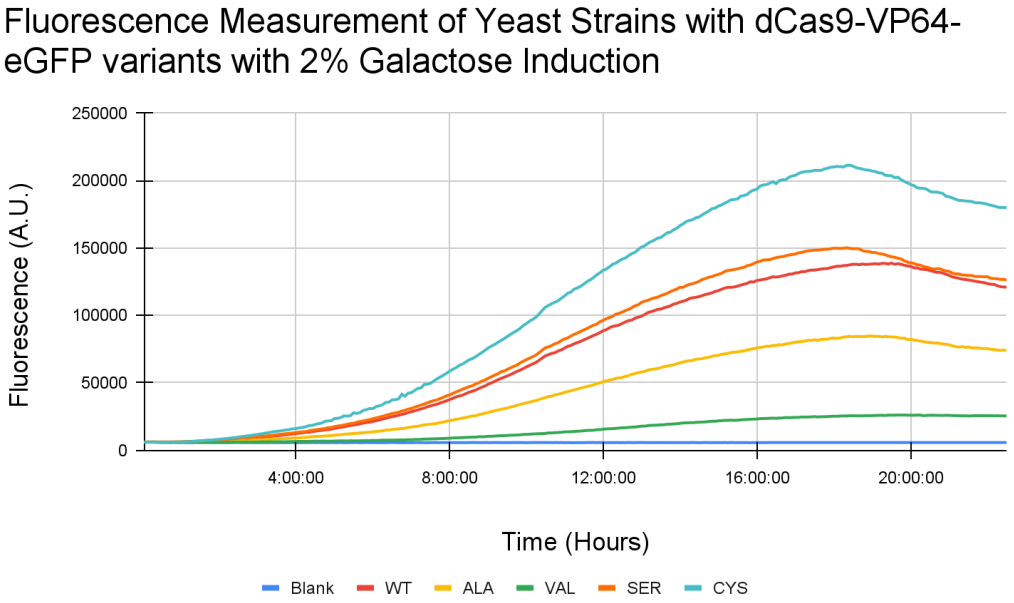

Figure 5. Fluorescent Curves of induced and non-induced dCas9-VP64 variants. A. All yeast transformants grown with 2% glucose, no cycloheximide, over 24 hours. Fluorescence recorded at 484 nm and 515nm **B.** All yeast transformants grown with 2% galactose, no cycloheximide, over 24 hours. Fluorescence recorded at 484nm and 515nm.

A

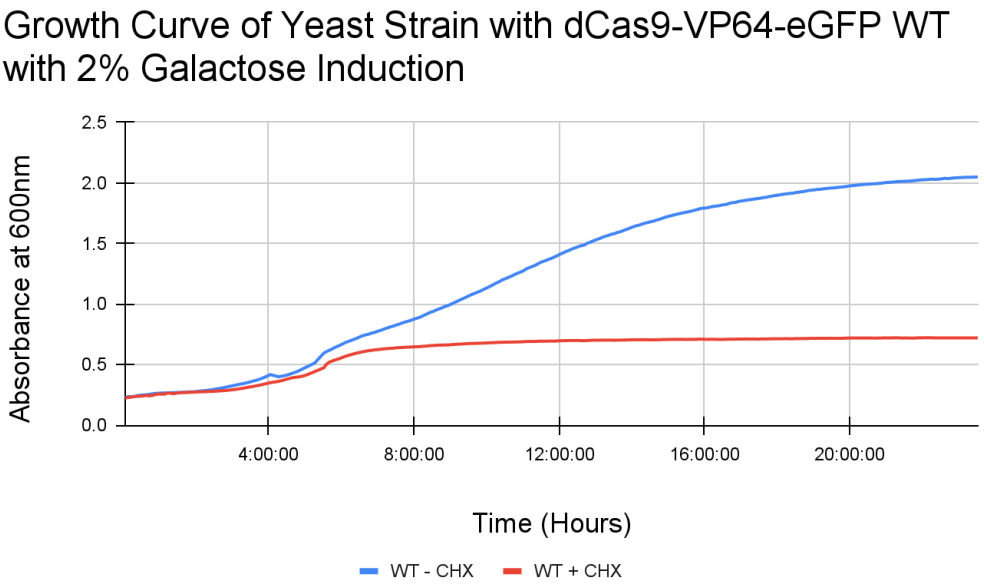

B

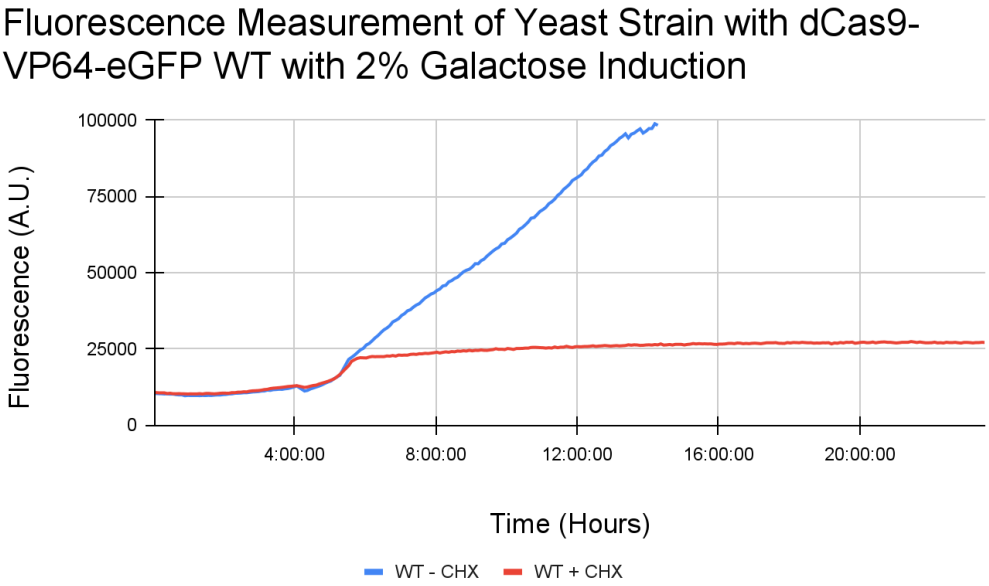

Figure 6. Growth and fluorescent curves of WT-dCas9-VP64-eGFP. A. Growth curve of induced wild type dCas9-VP64-eGFP with cycloheximide treated at time point 5 hours, untreated in blue, treated in red. **B.** Growth curve of induced wild type dCas9-VP64-eGFP with cycloheximide treated at time point 5 hours, untreated in blue, treated in red.

A

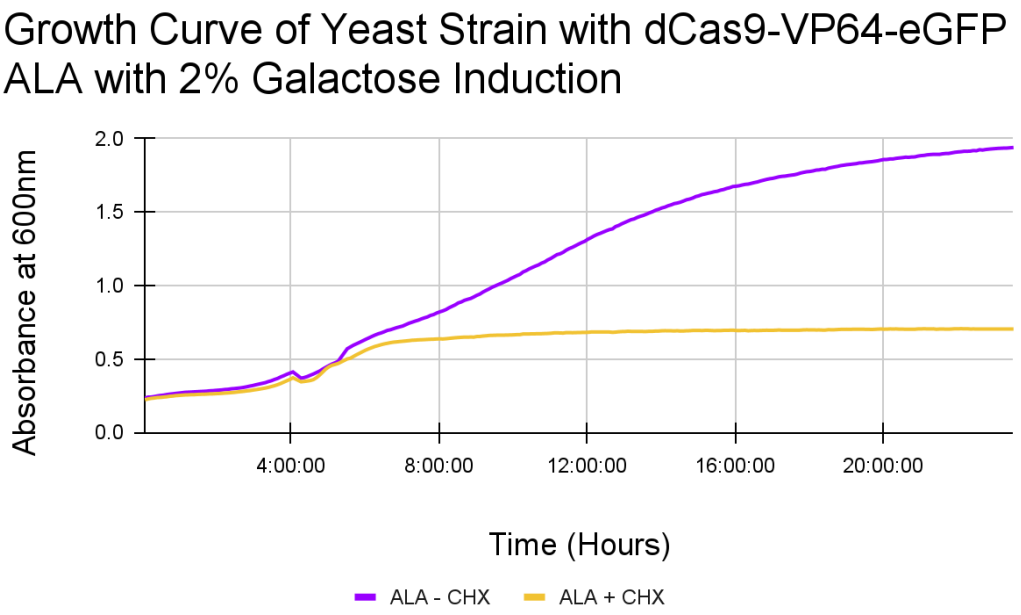

B

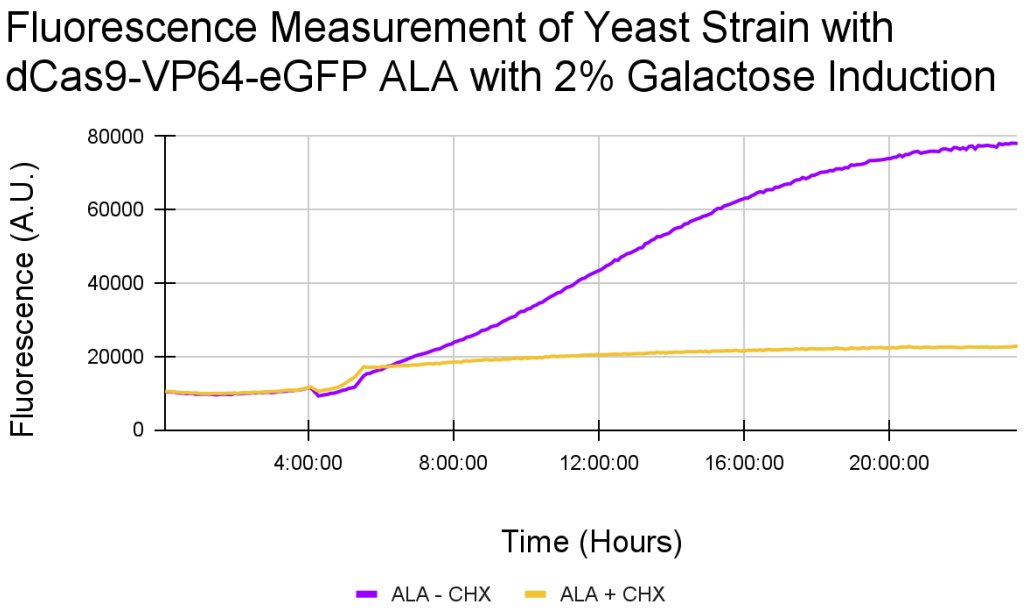

Figure 7. Growth and fluorescent curves of ALA-dCas9-VP64-eGFP. A. Growth curve of induced wild type dCas9-VP64-eGFP with cycloheximide treated at time point 5 hours, untreated in purple, treated in yellow. **B.** Growth curve of induced wild type dCas9-VP64-eGFP with cycloheximide treated at time point 5 hours, untreated in purple, treated in yellow.

A

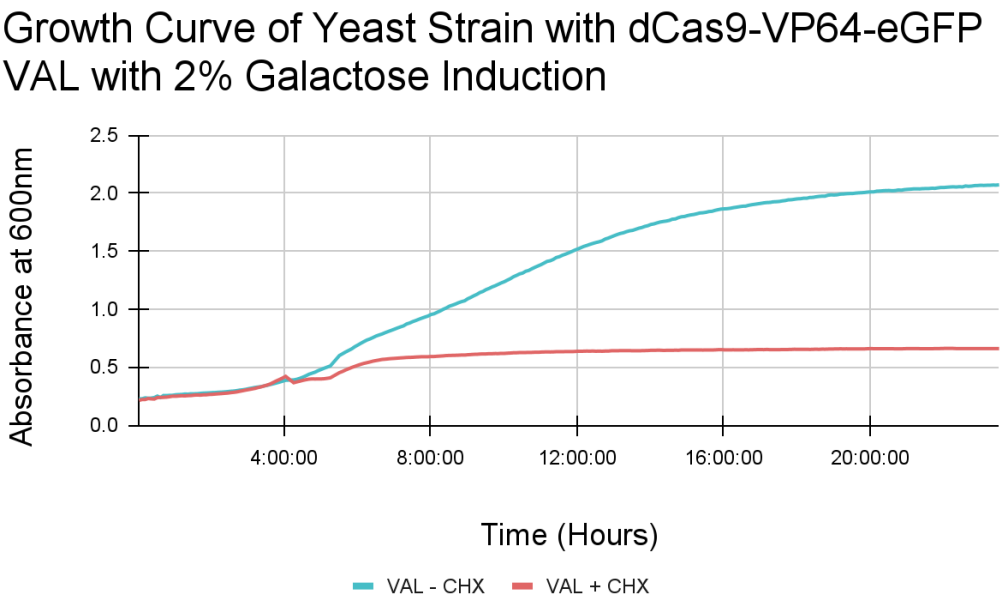

B

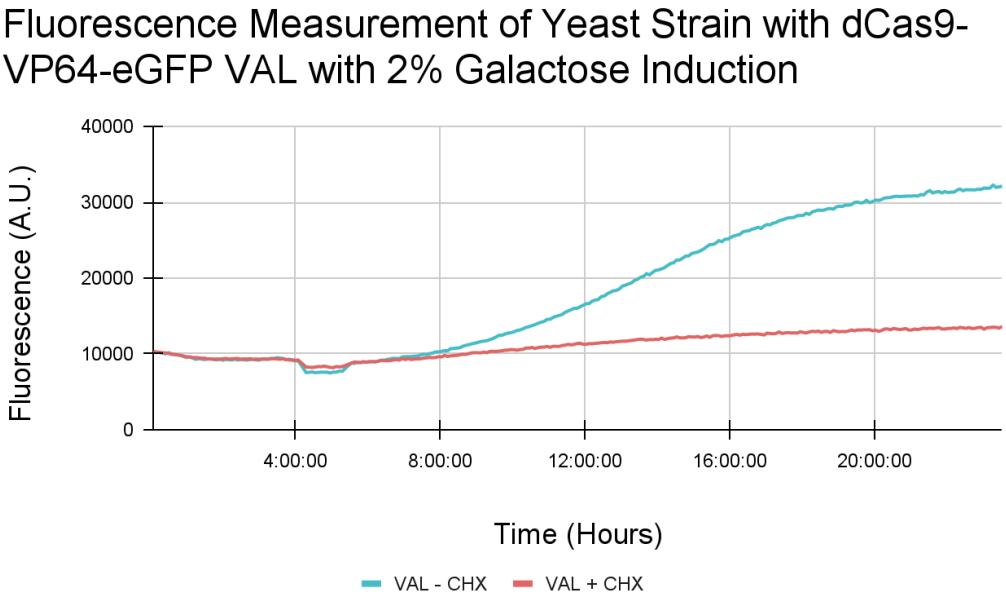

Figure 8. Growth and fluorescent curves of VAL-dCas9-VP64-eGFP. A. Growth curve of induced wild type dCas9-VP64-eGFP with cycloheximide treated at time point 5 hours, untreated in teal, treated in light red. **B.** Growth curve of induced wild type dCas9-VP64-eGFP with cycloheximide treated at time point 5 hours, untreated in teal, treated in light red.

A

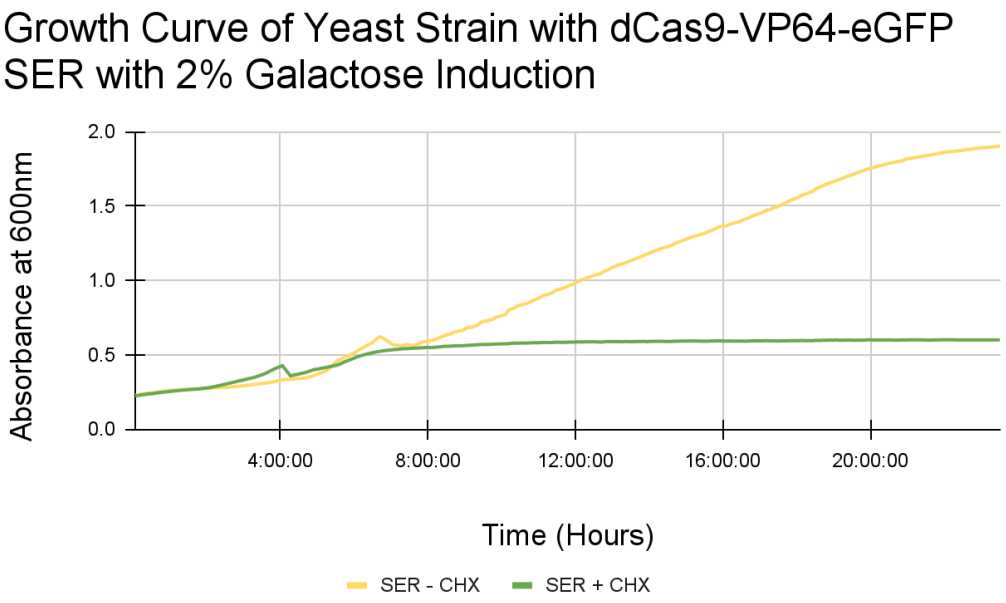

B

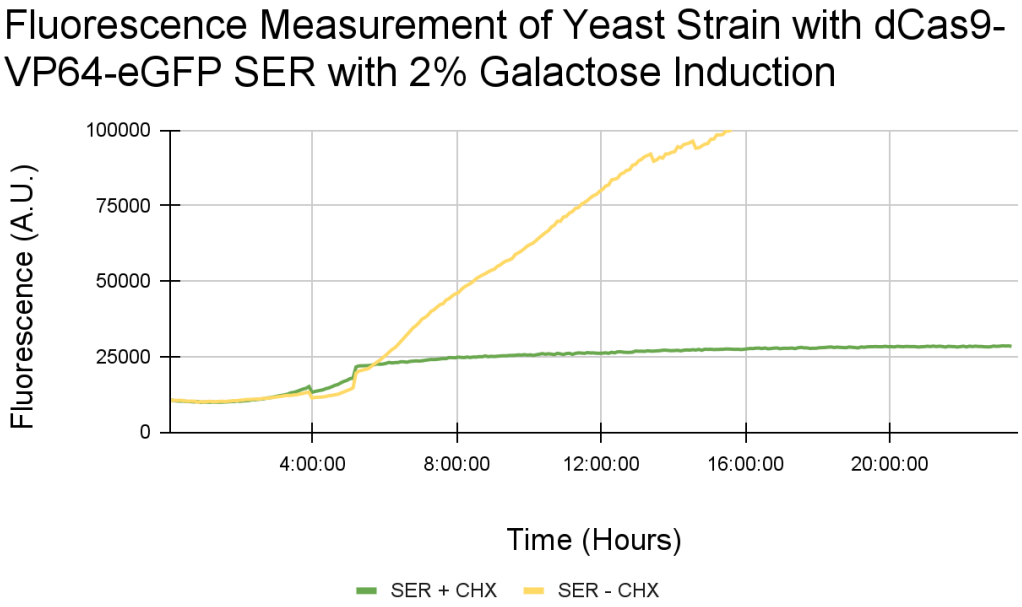

Figure 9. Growth and fluorescent curves of SER-dCas9-VP64-eGFP. A. Growth curve of induced wild type dCas9-VP64-eGFP with cycloheximide treated at time point 5 hours, untreated in yellow, treated in green. **B.** Growth curve of induced wild type dCas9-VP64-eGFP with cycloheximide treated at time point 5 hours, untreated in yellow, treated in green.

A

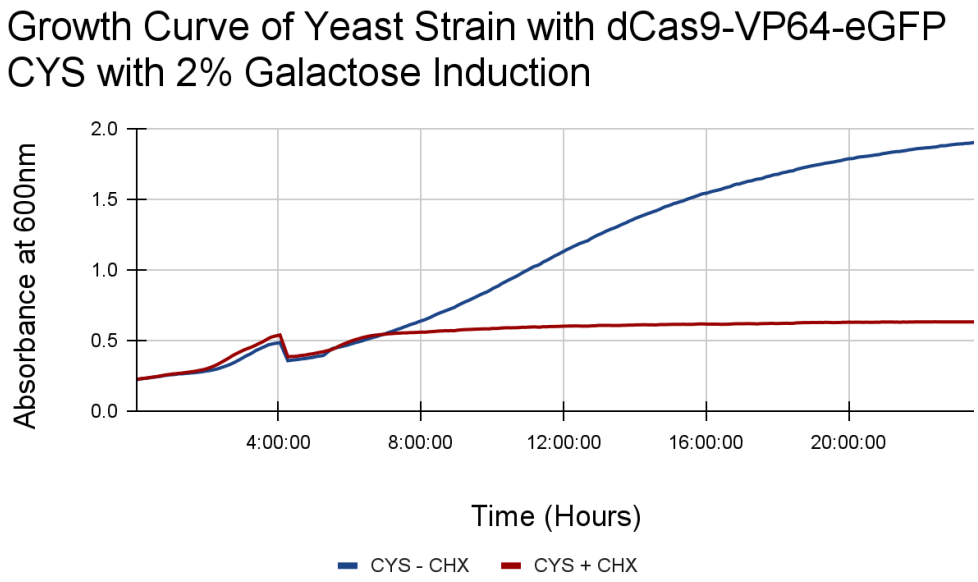

B

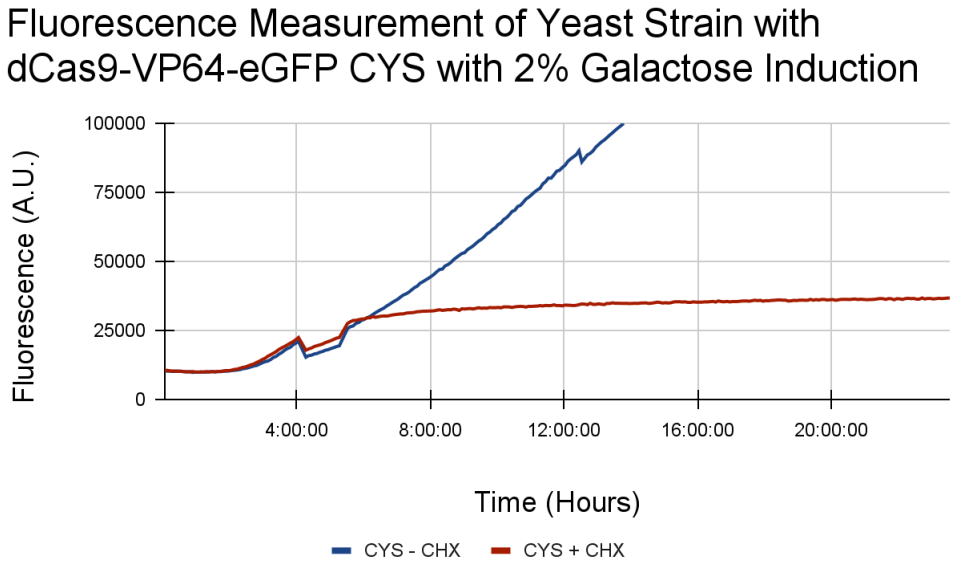

Figure 10. Growth and fluorescent curves of CYS-dCas9-VP64-eGFP. A. Growth curve of induced wild type dCas9-VP64-eGFP with cycloheximide treated at time point 5 hours, untreated in dark blue, treated in maroon. **B.** Growth curve of induced wild type dCas9-VP64-eGFP with cycloheximide treated at time point 5 hours, untreated in dark blue, treated in maroon.

Section 3: Galactose-1 promoter induces dCas9-VP64-eGFP levels based on the eGFP fluorescence

The fusion protein dCas9-VP64-eGFP was under the regulation of the galactose-1 promoter. Through induction, the protein can be tracked via eGFP fluorescence. The aim of this experiment was to confirm the eGFP signal and its localization by using fluorescent microscopy.

The experimental design of this experiment involved growing all variants under non-induced and induced conditions, to indicate that eGFP signal is produced in response to the galactose-1 promoter. The captured images clearly demonstrated that non-induced cells in 2% glucose lacked an eGFP signal, necessitating image oversaturation to visualize minimal green emission. In contrast, the variants induced in 2% galactose exhibited clear eGFP signals in the majority of cells, with a basal level of 50 nanoseconds of excitation (**Figure 11)**. However, the Valine N-term mutant did not show such induction; instead, it displayed basal levels similar to those seen in non-induced cultures. To visualize background signal of eGFP in the non-induced cells, a maxima signal enhancement was required. This confirmed that no production of eGFP occurred for cells under 2% glucose.

Additionally, at the center of a single body of the cells was a punctate signal of the eGFP which is consistent with the nuclear localization signal in the sequence of dCas9-VP64.

In summary, the microscopy data provides evidence of the successful inducible expression of dCas9-VP64-eGFP construct under the regulation of the Galactose 1 promoter.

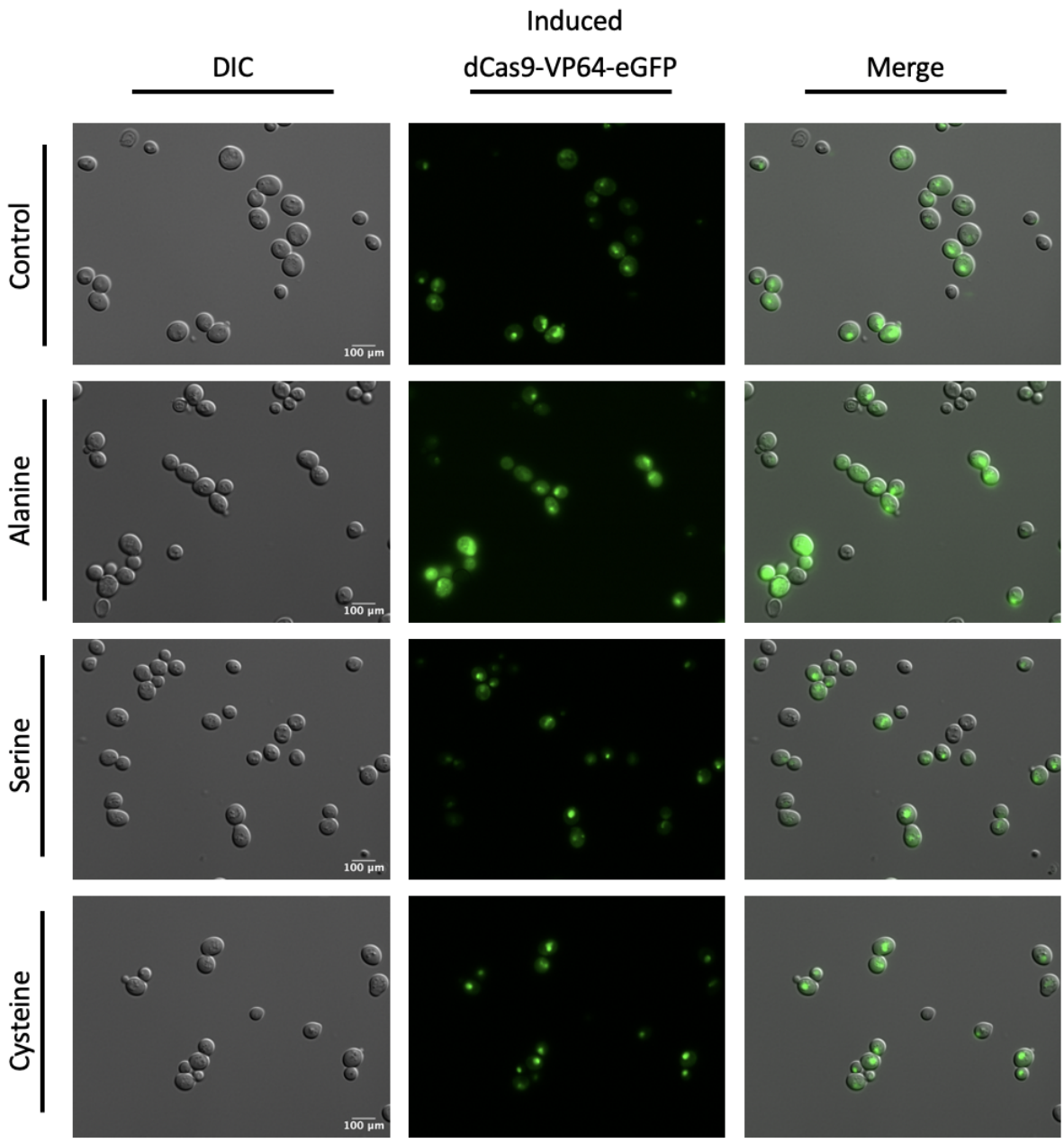

Figure 11. Fluorescent microscopy of uninduced and induced dCas9-VP64-eGFP variants. The images on the left are DIC of yeast strains in 2% glucose or 2% galactose media. The eGFP channel is in the middle. The right channel are the merged images of DIC and eGFP.

Section 4: The Cysteine Amino Acid Insertion on the dCas9-VP64-eGFP construct further reduces its half-life.

The study of protein degradation was completed by a cycloheximide assay that would inhibit protein synthesis and determine which N-terminal amino acid influenced the half-life of the dCas9-VP64 variants. The aim of this experiment was to load equal amounts of protein from each variant and track degradation of the eGFP signal over 2 hours once protein synthesis was inhibited.

The experimental design involved growing dCas9-VP64-eGFP, ALA-dCas9-VP64-eGFP, VAL-dCas9-VP64-eGFP, SER-dCas9-VP64-eGFP, CYS-dCas9-VP64-eGFP strains under induced conditions and treating with cycloheximide at mid log phase and conducting a western blot analysis to detect the decrease in eGFP fusion protein.

Figure 12 illustrates the detected levels of full fusion protein variants at 198 kDa, and their associated eGFP levels at 26.9 kDa. Glucose-6-phosphate dehydrogenase was used as a loading control to ensure that protein degradation was not a consequence of cell death, as its band intensity remained consistent throughout the time course for each variant protein lysis analysis. The negative control, which is untransformed wild-type *S. cerevisiae* BY4741, showed no signal for eGFP at 198 kDa and 26.9 kDa. This confirms the specificity of the eGFP antibody and validates that any detected signal is representative of the eGFP protein. Each variant had their respective lysed cells loaded at the same amount on a separate gel for glucose-6-phosphate dehydrogenase.

The WT-dCas9-VP64-eGFP transformant produced a band at 198 kDa protein of at time point 0 minutes. Over the course of cycloheximide treatment, there was a sharp decline in the WT-dCas9-VP64-eGFP, resulting in an approximate 60% decrease, as shown in the bar graph in **Figure 13**. Concurrently, the eGFP signal at 26.9 kDa, representing eGFP alone, increased during the degradation of WT-dCas9-VP64-eGFP, suggesting a buildup of non-degraded eGFP protein.

Notably, the wild-type variant displayed the highest initial signal compared to all other variants for the full-length WT-dCas9-VP64-eGFP protein.

The dCas9-VP64-eGFP alanine variant initiated at 50% of the wild type's initial signal and exhibited a similar degradation pattern for the full-length 198 kDa dCas9-VP64-eGFP. However, the eGFP signal at 26.9 kDa did not increase over time, suggesting that the full-length protein was potentially completely or in majority degraded together.

The serine variant started with an initial signal 80% lower for the full-length protein than that of the wildtype dCas9-VP64-eGFP signal. The serine variant followed a degradation rate like that of the wild-type and alanine variants. However, the eGFP signal at 26.9 kDa remained relatively unchanged over the two-hour period. The cysteine variant showed a similar signal intensity as the alanine variant at time point 0 for the full-length 198 kDa protein. However, the cysteine variant degraded faster than the other variants, with a signal decrease of approximately 80% at 30 minutes. The eGFP signal at 26.9 kDa showed an increase, comparable to the rate observed in the wild type eGFP detection.

Upon normalizing the band intensities and plotting them graphically, the first-order rate kinetic equation was applied to quantify the protein decay and determine their respective half-lives (**Figure 16**).

The wild-type variant exhibited a half-life of 57 minutes, the alanine variant had a half-life of 54 minutes, 5.25% faster than wild-type. The serine variant had a half-life of 61 minutes, 7% longer than wildtype. The cysteine variant had the shortest half-life of 37 minutes, 35% faster than wildtype (**Figure 17**). These results indicate that the N-terminal amino acid insertions, particularly the cysteine variant, effectively influenced the half-life of dCas9-VP64-eGFP.

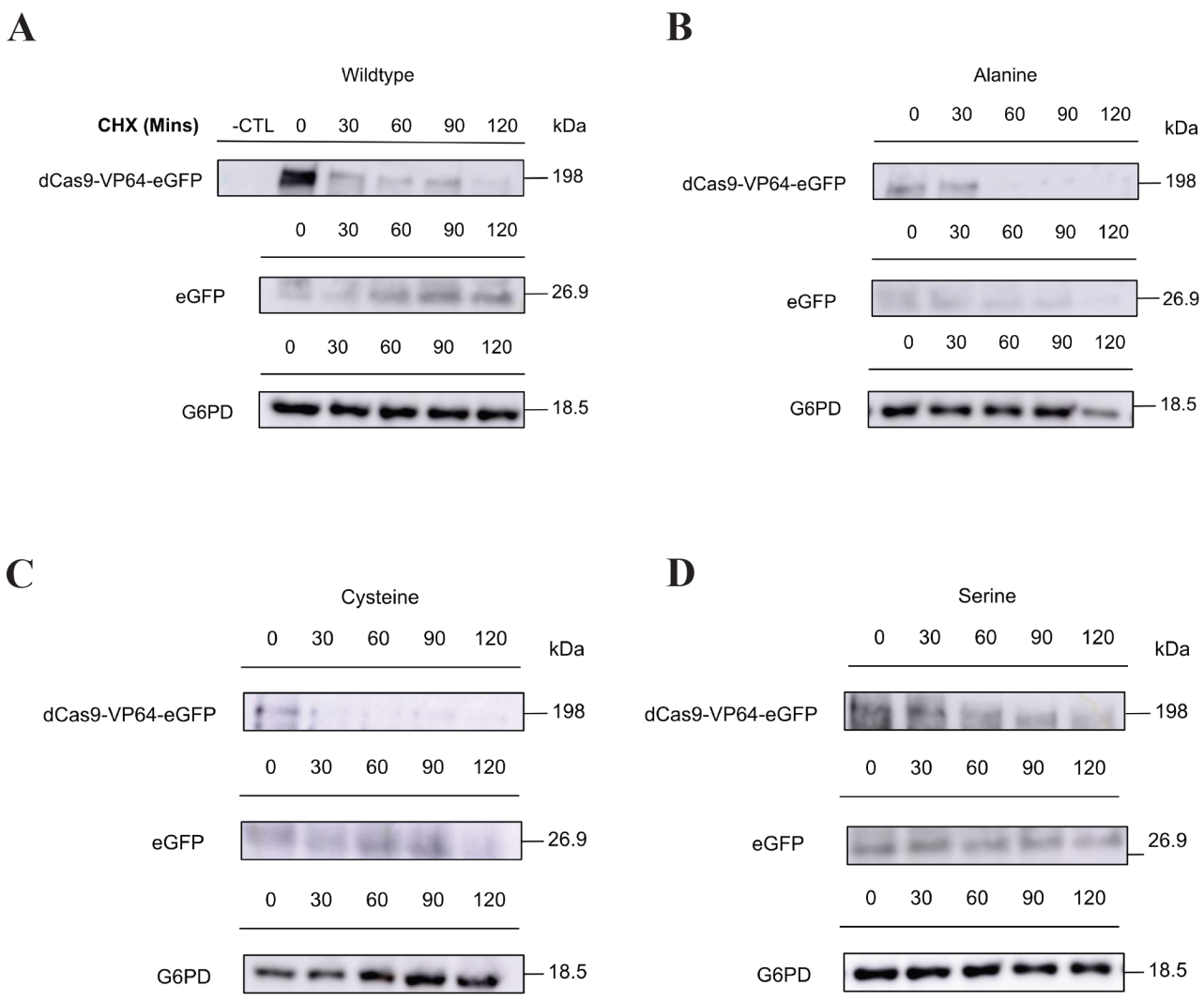

Figure 12. Western blot of full length dCas9-VP64-eGFP variants probed for eGFP during cycloheximide treatment. From left to right is the amount of time passed after CHX treatment at 0.25ug/mL. From top to bottom are dCas9-VP64-eGFP, eGFP and G6PD for all western blots. **A.** The western blot for the WT-dCas9-VP64-eGFP with the negative control in the far-left lane represents wildtype BY4741 yeast cells lysed. **B.** The western blot for the ALA-dCas9-VP64-eGFP **C.** The western blot for the CYS-dCas9-VP64-eGFP **D.** The western blot for the SER-dCas9-VP64-eGFP. The full length dCas9-VP64-eGFP is at 198 kDa, eGFP at 26.9kDa and the internal control at 18.5 kDa.

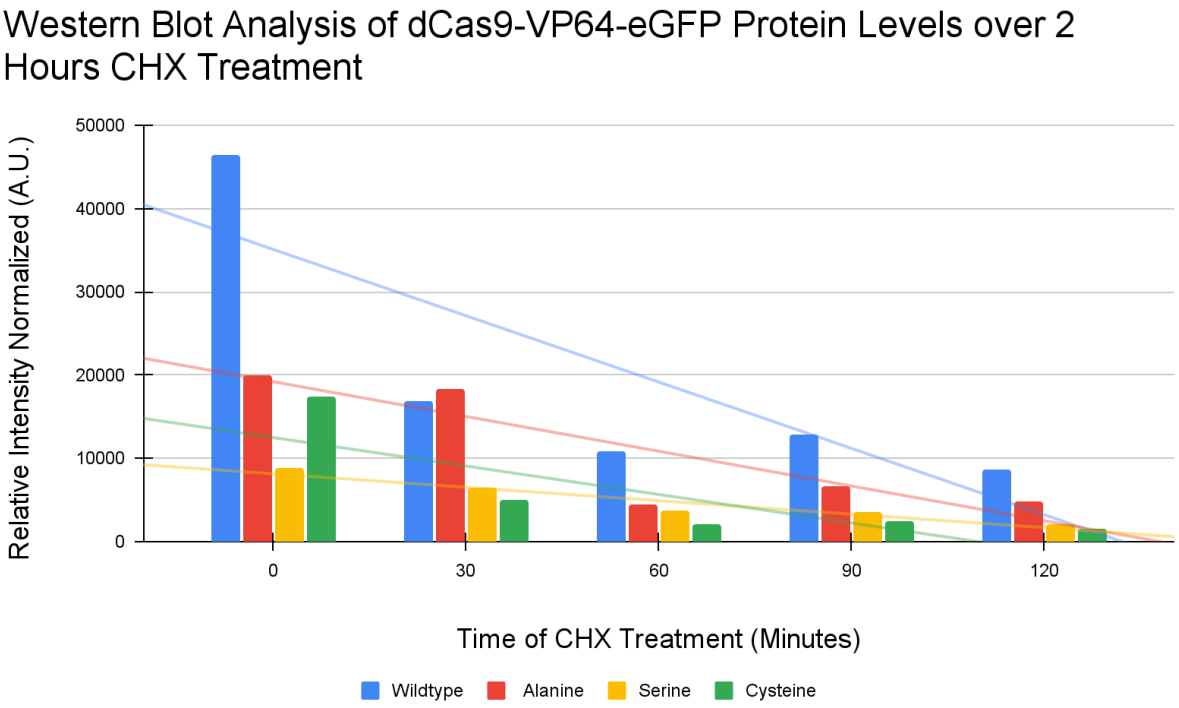

Figure 13. Western blot plot intensity analysis of all dCas9-VP64-eGFP variants during cycloheximide treatment. The western blot bands probed for eGFP were analyzed using the ImageJ gel analysis and normalized against the G6PDH control and plotted over two hours, representing protein decay. The linear regression line was used to identify the negative slope.

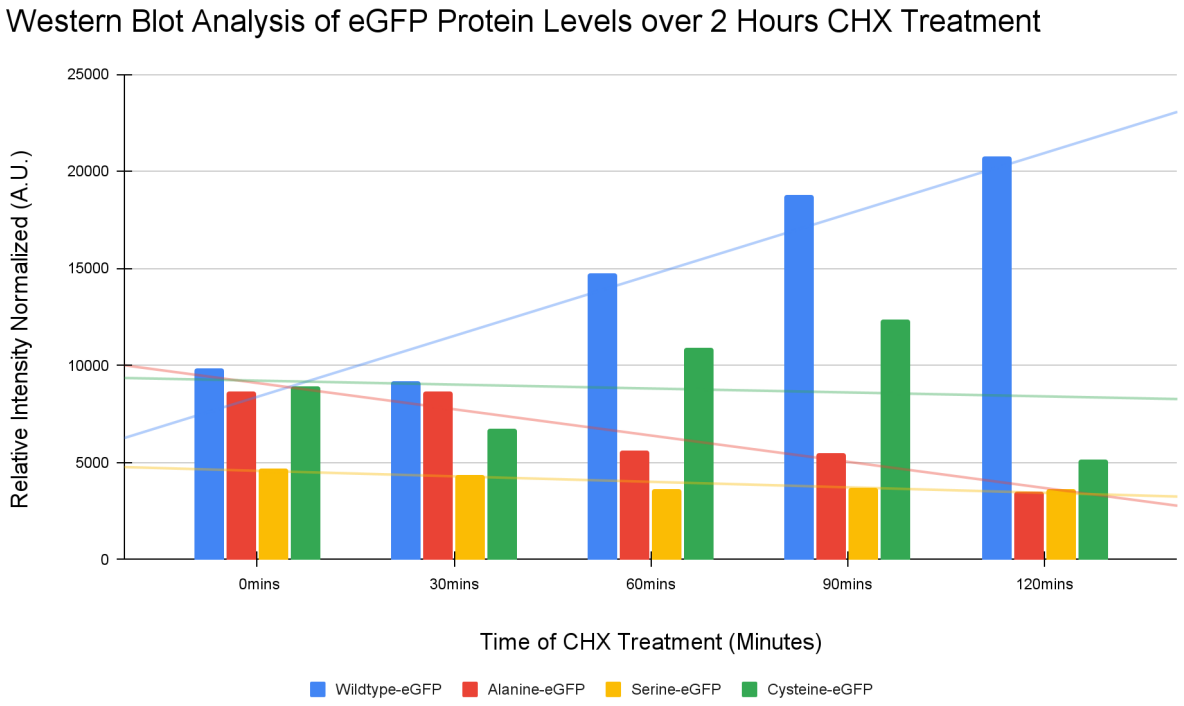

Figure 14. Western blot plot intensity analysis of eGFP signal from each variant during cycloheximide treatment. The western blot probed for eGFP was analyzed using the ImageJ gel analysis and normalized against the G6PDH control and plotted over two hours, representing protein decay. The linear regression line was used to identify the positive and negative slope.

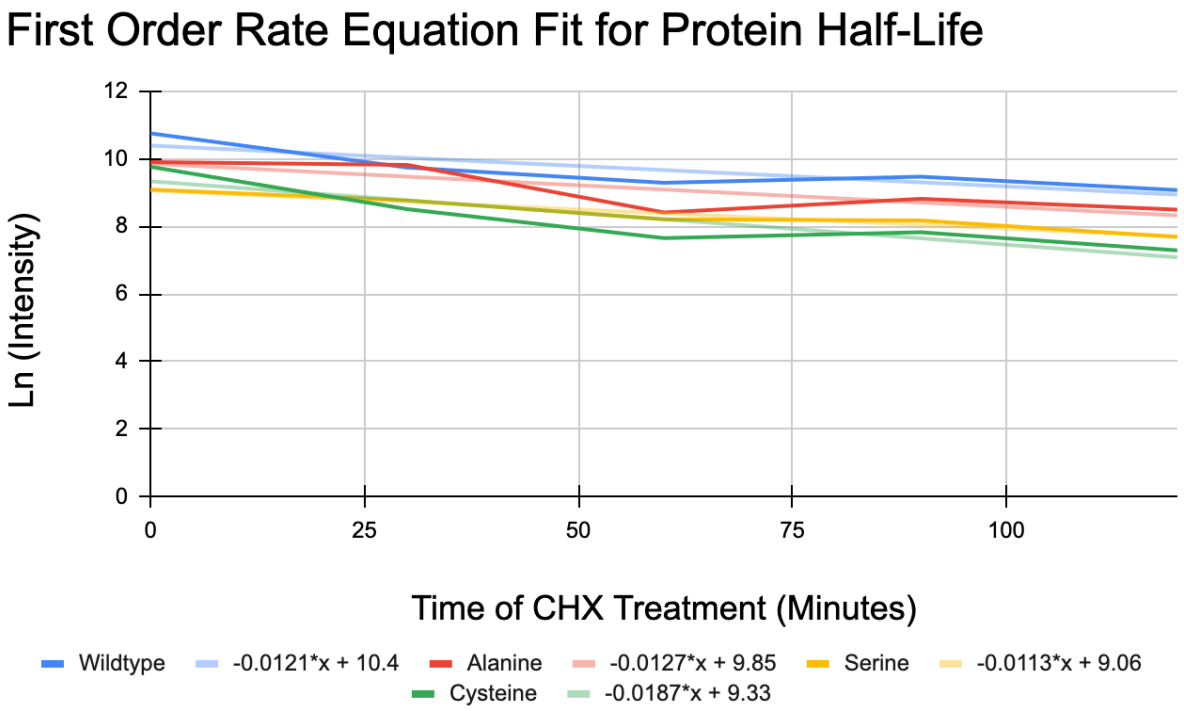

Figure 15. First order Rate Kinetic Curve for Protein Decay. The western blot band intensities are quantified for the constant degradation rate "k" and using the natural logarithm to identify the half-life.

Mutant N-Term	T ½ (Mins)
Wildtype	57
Alanine	54
Serine	61
Cysteine	37

$$First\ Order\ Rate\ Equation: T_{1/2} = \frac{Ln(2)}{k}$$

Figure 16. Half-Life of dCas9-VP64-eGFP Mutants. The half-life of each mutant in minutes using the natural logarithm of the first order rate kinetic equation, where "k" is the degradation rate constant (1/minute).

Section 5: Discussion

The study aimed to investigate how various N-terminal mutations affect the stability and expression of dCas9-VP64-eGFP. Based on the work of Varshavsky, we understood that several N-terminal amino acids can be N-acetylated which serves as a signal recognized by the Ubiquitin Proteasome System. This destabilization strategy was used to shorten the half-life of dCas9-VP64, where indirect monitoring via the fluorescent protein tag eGFP, would reveal the differential protein steady-state levels. Different mutations were introduced into the N-terminal region of the protein to indirectly assess their impact on protein turnover. The constructed variants included ALA-dCas9-VP64-eGFP, VAL-dCas9-VP64-eGFP, SER-dCas9-VP64-eGFP, and CYS-dCas9-VP64-eGFP. Sequencing and BLAST analysis confirmed the successful construction of these variants, maintaining a high degree of similarity to the wild-type dCas9-VP64 sequence (**Figure 3B**). When induced with 2% glucose, all variants exhibited a sigmoidal curve in their eGFP fluorescence, reaching their maxima after 12 hours of induction. However, when induced with 2% galactose, most variants achieved significantly higher fluorescence maxima, with the exception of VAL-dCas9-VP64-eGFP, which was comparable to glucose induction. CYS-dCas9-VP64-eGFP showed the highest fluorescence intensity, indicating enhanced protein expression (**Figure 4,5**). The difference in fluorescence signal production could be a result of the N-terminal amino acid change. In one study, a three amino acid change at the N-terminal of the protein caused it to have different folding kinetics. The researchers indicated that the extension influenced the folding kinetics and denaturation equilibrium (Korepanova A., 2001). Comparing these findings to the N-terminal changes on the dCas9-VP64-eGFP, there is a potential folding difference leading up to higher fluorescence detected.

The growth curves also revealed differences in growth parameters between glucose and galactose induction. This potentially indicates that the strains harboring the plasmid have undergone stress to produce the large protein, dCas9-VP64-eGFP. Literature has shown that recombinant proteins can vary the growth kinetics because the translation of the protein is metabolically taxing. The transcription and translation rate can be influenced by the presence of large recombinant proteins (Li Z. & Rinas U., 2020). Microscopy data confirmed the successful inducible expression of dCas9-VP64-eGFP constructs under the regulation of the Galactose 1 promoter. Cells induced with galactose exhibited clear eGFP signals, while those in glucose did not produce detectable eGFP signals. Additionally, the punctate eGFP signal within the cells was consistent with nuclear localization, as expected. To confirm that the protein is in the nucleus, a co-staining of the cells with DAPI, a DNA dye, could reveal overlapping signals of eGFP and DAPI through fluorescent microscopy (Kapuscinski J., 1995).

To assess the impact of N-terminal mutations on protein stability, a cycloheximide assay was conducted to inhibit protein synthesis and measure eGFP signal decay over 2 hours. Cycloheximide is a fungicide used to block protein synthesis by binding to the ribosome and is a common method to studying protein turnover (Schneider-Poetsch, 2010). Western blot analysis showed that wild-type dCas9-VP64-eGFP had a half-life of 57 minutes. The alanine variant had a slightly shorter half-life (54 minutes), while the serine variant had a longer half-life (61 minutes). Notably, the cysteine variant exhibited the shortest half-life (37 minutes), indicating faster protein turnover (**Figure 16**). Furthermore, as seen by **Figure 14**, we observed that there is an accumulation of eGFP during the degradation of the full length dCas9-VP64-eGFP for wildtype and cysteine variants, while alanine and serine did not demonstrate a build-up. This could potentially mean that during the degradation of the dCas9-VP64 and upon cleavage of the peptide

separating it from the eGFP, the fluorescent protein remained stable enough and folded, allowing for its detection. This was seen by the microplate reader (**Figures 6-10**), where the signal did not decrease over 24 hours. This data would agree with the increasing signal of eGFP alone on the western blot of wild type and cysteine (**Figure 12, 14**). It has been previously shown that GFP resisted proteasomal degradation and only partial degradation of the protein was observed (Khmelinskii A. et al., 2016).

These findings have implications for understanding how specific N-terminal mutations can modulate the stability and expression of dCas9-VP64-eGFP. The variations observed in eGFP fluorescence and protein half-lives among the different variants suggest that N-terminal mutations can be a valuable tool for fine-tuning protein expression and stability. This knowledge could be applied to optimize the design of genetic circuits and synthetic biology applications.

Building upon these results, several promising future directions can be pursued to advance genetic tools with shorter half-lives. One potential avenue is the incorporation of tandem cysteine units at the N-terminus of dCas9-VP64. Previous studies have demonstrated that tandem degrons can promote destabilization at the sequence level and effectively at the peptide level (Ole K Tørresen et al., 2019). This could support the investigation that multiple cysteine residues in succession could further destabilize the protein and achieve even shorter half-lives.

Another direction involves the inhibition of the proteasome. This could fortify the hypothesis that N-terminal amino acids that are N-acetylated are specifically degraded by the UPS pathway and not others such as lysosomal degradation. Verify that once the proteasome is inhibited, can dCas9-VP64 still be produced and detected. In addition to this, a strategy to accelerate degradation would be through fusing the N-terminus of dCas9-VP64 with a ubiquitin tag, specific E3 ligases from the UPS could be recruited to initiate protein degradation (Komander

& Rape, 2012). Given the affinity of these residues to the E3 ligases, an increase in protein turnover can be observed. An important one would be to test the functionality of the short half-life dCas9-VP64 and combine within the construct a gRNA to target a reporter gene.

Furthermore, integrating the N-end rule strategy with oscillatory genetic circuits offers the potential to create highly sophisticated gene regulation systems. By combining the rapid turnover of dCas9-VP64 achieved through the N-end rule and potentially other added N-degrons, periodic gene expression patterns of oscillatory circuits can be achieved. Researchers could develop novel genetic networks capable of precise and dynamic control of gene expression over time (Kuo J. et al., 2020). This integration could open new avenues for designing oscillating genetic circuits with applications in various biological processes and therapeutic interventions.

In conclusion, the investigation of shorter half-lives through the N-end rule pathway has provided valuable insights into the potential for achieving dynamic and tightly regulated gene expression with genetic engineering tools such as dCas9-VP64. The results highlight the significance of the N-terminus in governing protein degradation and its potential to be further explored as an artificial strategy to predicting half-lives. While the cysteine variant exhibited a significantly shorter half-life, future directions, such as tandem cysteine units, ubiquitin tagging, proteasome inhibition, and integration with oscillatory circuits with gRNA, hold great promise for advancing and enhancing their applications in synthetic biology, biotechnology, and gene therapy. By harnessing these strategies, researchers can unlock new possibilities for precise and dynamic gene regulation, paving the way for innovative biomedical and biotechnological advancements.

Section 6: Materials and Methods

6.1. Strains and Media

All *Escherichia coli* strains transformed with wild-type and mutant N-terms of the dCas9-VP64-eGFP construct were grown in Luria Broth Base (ThermoFischer Scientific, 12795027) with 100 ug/mL Ampicillin or 50 ug/mL Kanamycin. The *E. coli* used in transformations were ordered from the NEB® 5-alpha Competent *E. coli* High Efficiency kit (New England Biolabs, C2987H). The *E. coli* cells were miniprepped with the GeneJET Plasmid miniprep kit (ThermoFischer, K0502)

The haploid *Saccharomyces cerevisiae* strain BY4741 with the genotype *MATa his3Δ1 leu2Δ0 met15Δ0 ura3Δ0,* provided from the Kachroo Lab, was used for transformation of all dCas-VP64-eGFP constructs. The yeast cells were made competent and transformed using the Frozen-EZ Yeast Transformation II kit (Zymogen, T2001). Transformation of the yeast cells was completed by incubating the cells with 1ug of DNA of the assembled construct. The yeast cells were grown in Yeast Synthetic-Depleted Uracil media with the following components from Sigma Aldrich: Dextrose (2% w/v), Galactose (2% w/v), L-Glutamic Acid (1.2g/L), yeast synthetic drop-out medium supplements without uracil (1.92g/L).

6.2. Site-Directed Mutagenesis and Gateway Cloning

The yeast codon optimized dCas9-VP64 gene was used from the Addgene vector #49013. A forward primer was designed to include the 3 base pair insertion on the 5' end and a reverse primer to anneal directly to the template (Oligonucleotides in Supplementary Information). A PCR amplification of the site-directed mutated vector was done using the Q5® High-Fidelity DNA

Polymerase (New England BioLab, M0491S) with the following conditions: initial denaturation at 98 °C for 30 seconds, 35 cycles at 98 °C for 10 seconds, annealing at 54 °C for 30 seconds, extension 72 °C for 5 minutes and 30 seconds, final extension 72 °C for 10 minutes and hold at 4 °C indefinitely. From the PCR product, 1uL was added to a KLD reaction mix (New England BioLab, M0554S), containing kinase, ligase and DpnI restriction enzyme. The reaction mix was incubated at room temperature for 1 hour and 5uL was used in the transformation of high efficiency *E. coli* competent cells. Each transformant was miniprepped for the site-directed mutagenic plasmid as previously described.

Hybrid primers were designed to flank the N-terminus mutation of the dCas9-VP64 gene with added attB sites for cloning into the Gateway™ pDONR™221 vector (ThermoFisher Scientific, 12536017). The Gateway cloning reaction included: 600 ng of PCR product, 150 ng of pDONR221 vector, 1X TE Buffer up to a final volume of 8uL. The reaction mix would then include 1uL of Gateway™ BP Clonase™ II Enzyme mix (ThermoFisher Scientific, 11789020) and incubated at room temperature overnight. After incubation, 1uL of Proteinase K (Thermofischer Scientific, EO0491) is added to the mix, incubated at 37 °C for 10 minutes, transformed in to One Shot™ ccdB Survival™ 2 $T1^R$ Competent Cells (Invitrogen, A10460) and plated on LB Kan+ agar. The pDONR221- dCas9-VP64 colonies are inoculated and miniprepped as previously described. The final Gateway Cloning reaction consisted of: 150ng of pDONR221-dCas9-VP64 DNA variants, 450ng of pAG416-ccdb-eGFP destination vector, 1uL Gateway™ LR Clonase™ II Enzyme mix, (ThermoFisher Scientific, 11791020), 1X TE Buffer up to a final volume of 8uL. The reaction mix was incubated, stopped with Proteinase K and transformed into *ccd*B resistant *E. coli* cells as previously described.

6.3. Fluorescence Micro-plate Reader based Cycloheximide Chase Assay

The strains expressing the dCas9-VP64-eGFP were inoculated in 10 mL of SD-URA 2% glucose overnight. The next day, equal volumes of the culture would be split in to two flacon tubes and centrifuged at 3500 RPM at 23 °C for 10 minutes. Each variant would have one pellet resuspended in 5mL of fresh SD-URA 2% glucose and the other pellet resuspended in SD-URA 2% galactose. The optical density at 600 nm of each culture would be measured and used for normalization into a next set of fresh media of SD-URA 2% glucose and 2% galactose. A back dilution to an OD600 of 0.2 would be completed by using the following formula: desired OD/Sample OD = % of sample in final volume. From each culture, 200uL would be place in a 96-well black transparent bottom Nunc plate, in triplicates. For each variant, 6 wells would have the same strain under the same conditions, 3 of which be treated with cycloheximide at an OD600nm of 0.6-0.8. The plate is placed in the BioTek Synergy H1 microplate reader with an excitation wavelength of 485 nm and an emission wavelength of 515 nm, while simultaneously recording the absorbance at 600nm, with continuous linear shaking, at 30 °C. The fluorescence and growth would be recorded every 5 minutes over 23 hours. At time point 5 hours, where optical density would be around 0.6-0.8, the plate would come out and cycloheximide (Sigma-Aldrich, C4859) would be added to three wells at a concentration of 0.25ug/mL.

6.4. Live Cell Fluorescence Microscopy

To verify that induction in galactose media is producing a fluorescence signal of eGFP in the cells, the strains were inoculated overnight in two cultures, SD-URA 2% glucose and SD-URA 2% galactose. The cells would be back diluted, as previously described, to an OD600 of 0.5.

Induced and uninduced cell images would be captured using the Leica DMI6000 inverted microscope programmed with the volocity software with DIC optics and fluorescent GFP laser emission at 485 nm and 515 nm.

6.5. Protein Lysates and Western Blots

All yeast strains underwent a chemical and mechanical lysis protocol adapted from Yang et al. 2020, to allow solubilized protein content for western blot analysis. Cultures were grown overnight at 30 °C shaking at 200 RPM in SD-URA 2% glucose. The cultures were then back diluted the morning after to an OD600 of 0.4, using the formula previously described and a final volume of 10mL of fresh SD-URA 2% galactose. The cells would be pelleted at 3,500 RPM for 5 minutes at room temperature. Over the course of 3 hours, the OD600 is recorded until the culture reaches an OD600 of 0.6-0.8. Once in log phase, 1 OD unit is collected by using this formula: 1/current OD600 = Volume of culture for 1 OD600 Unit. This method is used to normalize the number of cells collected for lysis. A cell count is also completed to verify.

At time point 0 hrs, 1 OD600 unit is collected and pelleted for lysis and the cycloheximide (Sigma-Aldrich, C4859) is added to the rest of the culture at a concentration of 0.25ug/mL and kept incubated at 30 °C shaking at 200 RPM until the next lysis point. The supernatant is removed, and the pellet is resuspended in 2X Boiling Buffer (1.5M Tris, 0.5M EDTA, 10%SDS) with 2uL of Protease Inhibitor Cocktail (Cell Signalling Technology, 5871S). Around 100uL of 0.5mm diameter Zircomia/Silica beads (BioSpec, 11079105z) is added and the mix is subjected to the Disruptor Genie for 5 minutes (Scientific Industries). The cell suspension is then transferred to a heating block at 65 °C for 5 minutes. After incubation, 100uL of the 2X Urea Buffer (150mM Tris, 6M Urea, 6% SDS, 40% Glycerol, 0.01% Bromophenol Blue, 100mM DTT. It is then re-subjected

to 5 minutes of disruption and 5 minutes of heating and used for loading onto a gel. This was repeated for each variant at a lysis point of t=0 mins of cycloheximide incubation, t=30 mins, t=60 mins, t=90 mins, t=120 mins, where 1OD unit was collected at each point.

Equal amounts of protein lysates were gel-electrophoresed on a Mini-Protean TGX^{TM} 10% SDS-Polyacrylamide gel (BioRad, 456-1036) for 1 hour at 150 volts. The proteins were transferred onto a nitrocellulose membrane using the Trans-Blot Turbo Transfer System (BioRad). The membrane was Ponceau Stained and washed 3 times with distilled water before blocking with 5% milk in TBST (1% Tween-20) for 1 hour. The blots were incubated either with primary anti-Green Fluorescent Protein, Mouse-IgG, monoclonal antibody (Sigma-Aldrich, 11814460001) at a 1:1000 dilution or in anti-Glucose-6-Phosphate Dehydrogenase, Rabbit-IgG, polyclonal antibody (Sigma-Aldrich, A9521-1VL) at a dilution of 1:15 000, shaking for 1 hour. The blots probed for GFP were conjugated with a secondary Goat Anti-Mouse IgG (H+L) Peroxidase antibody (SeraCare, 5220-0341) at a dilution of 1:5000. The blots probed for glucose-6-phosphate dehydrogenase were conjugated with a secondary Goat Anti-Rabbit IgG Peroxidase antibody (SeraCare, 5450-0010) at a dilution of 1:5000. The western blot was visualized using chemiluminescence with the Amersham™ ECL™ Prime Western Blotting Detection Reagent (Fisher Scientific, RPN2232) and the AI600 Chemiluminescent Imager (GE). The ImageJ software was used to quantify the band intensities and normalize them against the internal control glucose-6-phosphate dehydrogenase. Following the normalization, the intensities were fitted to the first-order rate constant equation $T1/2 = \ln(2)/k$. This plot determined the rate at which the protein degrades in minutes.

Section 7: References

- "Fluorescence Microplate-Based Cycloheximide Chase Assay: A Technique to Monitor the Degradation Kinetics of Fluorescent Nuclear Misfolded Proteins." *Protocol*, www.jove.com/v/21224/fluorescence-microplate-based-cycloheximide-chase-assay-technique-to. Accessed 13 Sept. 2023.

- Aksnes, H., Van Damme, P., Goris, M., Starheim, K. K., Marie, M., Støve, S. I., ... & Arnesen, T. (2015). An organellar Nα-acetyltransferase, naa60, acetylates cytosolic N termini of transmembrane proteins and maintains Golgi integrity. Cell Reports, 10(8), 1362-1374.

- Arnesen, T. Protein N-terminal acetylation: NAT 2007–2008 Symposia. BMC Proc 3 (Suppl 6), S1 (2009). https://doi.org/10.1186/1753-6561-3-S6-S1

- Arnesen, T., Van Damme, P., Polevoda, B., Helsens, K., Evjenth, R., Colaert, N., Varhaug, J. E., Vandekerckhove, J., Lillehaug, J. R., Sherman, F., Gevaert, K. (2009). Proteomics analyses reveal the evolutionary conservation and divergence of N-terminal acetyltransferases from yeast and humans. Proceedings of the National Academy of Sciences of the United States of America, 106(20), 8157–8162.

- Balboa D, Weltner J, Eurola S, Trokovic R, Wartiovaara K, Otonkoski T. Conditionally Stabilized dCas9 Activator for Controlling Gene Expression in Human Cell Reprogramming and Differentiation. Stem Cell Reports. 2015 Sep 8;5(3):448-59. doi: 10.1016/j.stemcr.2015.08.001. PMID: 26352799; PMCID: PMC4618656.

- Bard JAM, Goodall EA, Greene ER, Jonsson E, Dong KC, Martin A. Structure and Function of the 26S Proteasome. Annu Rev Biochem. 2018 Jun 20;87:697-724. doi: 10.1146/annurev-biochem-062917-011931. Epub 2018 Apr 13. PMID: 29652515; PMCID: PMC6422034.

- Belle, Archana, et al. "Quantification of protein half-lives in the budding yeast proteome." Proceedings of the National Academy of Sciences, vol. 103, no. 35, 2006, pp. 13004–13009, https://doi.org/10.1073/pnas.0605420103.

- Berndt J, Kovacs P, Ruschke K, Klöting N, Fasshauer M, Schön MR, Körner A, Stumvoll M, Blüher M. Fatty acid synthase gene expression in human adipose tissue: association with obesity and type 2 diabetes. Diabetologia. 2007 Jul;50(7):1472-80. doi: 10.1007/s00125-007-0689-x. Epub 2007 May 11. PMID: 17492427.

- Casas-Mollano JA, Zinselmeier MH, Erickson SE, Smanski MJ. CRISPR-Cas Activators for Engineering Gene Expression in Higher Eukaryotes. CRISPR J. 2020 Oct;3(5):350-364. doi: 10.1089/crispr.2020.0064. PMID: 33095045; PMCID: PMC7580621.

- Charis L Himeda, Takako I Jones, Peter L Jones, CRISPR/dCas9-mediated Transcriptional Inhibition Ameliorates the Epigenetic Dysregulation at D4Z4 and Represses DUX4-fl in FSH Muscular Dystrophy, Molecular Therapy, Volume 24, Issue 3, 2016, Pages 527-535, ISSN 1525-0016, https://doi.org/10.1038/mt.2015.200.

- Clute, Paul and Julian G. Pines. "Temporal and Spatial Control of Cyclin B1 Destruction in Metaphase." Nature Cell Biology, vol. 1, no. 2, 1999, pp. 82-87.

- Duan J, Sun L, Huang H, Wu Z, Wang L, Liao W. Overexpression of fatty acid synthase predicts a poor prognosis for human gastric cancer. Mol Med Rep. 2016 Apr;13(4):3027-35. doi: 10.3892/mmr.2016.4902. Epub 2016 Feb 17. PMID: 26936091; PMCID: PMC4805063.

- Eagle LR, Yin X, Brothman AR, Williams BJ, Atkin NB, Prochownik EV. Mutation of the MXI1 gene in prostate cancer. Nat Genet. 1995 Mar;9(3):249-55. doi: 10.1038/ng0395-249. PMID: 7773287.

- Finley, Daniel. "Recognition and processing of ubiquitin-protein conjugates by the proteasome." Annual Review of Biochemistry, vol. 78, 2009, pp. 477-513.

- Gilbert LA, Larson MH, Morsut L, Liu Z, Brar GA, Torres SE, Stern-Ginossar N, Brandman O, Whitehead EH, Doudna JA, Lim WA, Weissman JS, Qi LS. CRISPR-mediated modular RNA-guided regulation of transcription in eukaryotes. Cell. 2013 Jul 18;154(2):442-51. doi: 10.1016/j.cell.2013.06.044. Epub 2013 Jul 11. PMID: 23849981; PMCID: PMC3770145.

- Gilbert, L. A., Larson, M. H., Morsut, L., Liu, Z., Brar, G. A., Torres, S. E., ... & Qi, L. S. (2014). CRISPR-mediated modular RNA-guided regulation of transcription in eukaryotes. Cell, 154(2), 442-451.

- Goldberg, A. L. (2003). Protein degradation and protection against misfolded or damaged proteins. Nature, 426(6968), 895–899.

- Groll, Michael, et al. "A gated channel into the proteasome core particle." Nature Structural Biology, vol. 7, no. 11, 1997, pp. 1062-1067.

- Haugwitz, M., Garachtchenko, T., Nourzaie, O. et al. Rapid, on-demand protein stabilization and destabilization using the ProteoTuner™ systems. Nat Methods 5, iii–iv (2008). https://doi.org/10.1038/nmeth.f.223

- Hershko, A., Ciechanover, A. (1998). The ubiquitin system. Annual Review of Biochemistry, 67, 425–479.
- Hole K, Van Damme P, Dalva M, Aksnes H, Glomnes N, Varhaug JE, Lillehaug JR, Gevaert K, Arnesen T. The human N-alpha-acetyltransferase 40 (hNaa40p/hNatD) is conserved from yeast and N-terminally acetylates histones H2A and H4. PLoS One. 2011;6(9):e24713. doi: 10.1371/journal.pone.0024713. Epub 2011 Sep 15. PMID: 21935442; PMCID: PMC3174195
- Horton JD, Goldstein JL, Brown MS. SREBPs: activators of the complete program of cholesterol and fatty acid synthesis in the liver. J Clin Invest. 2002 May;109(9):1125-31. doi: 10.1172/JCI15593. PMID: 11994399; PMCID: PMC150968.
- Hsu, P. D., Scott, D. A., Weinstein, J. A., Ran, F. A., Konermann, S., Agarwala, V., ... & Zhang, F. (2013). DNA targeting specificity of RNA-guided Cas9 nucleases. Nature biotechnology, 31(9), 827-832.
- Hwang, C. S., Shemorry, A., & Varshavsky, A. (2003). N-terminal acetylation of cellular proteins creates specific degradation signals. Science, 327(5968), 973-977.
- Javaid N, Pham TLH, Choi S. Functional Comparison between VP64-dCas9-VP64 and dCas9-VP192 CRISPR Activators in Human Embryonic Kidney Cells. Int J Mol Sci. 2021 Jan 1;22(1):397. doi: 10.3390/ijms22010397. PMID: 33401508; PMCID: PMC7795359.

- Jinek M, Chylinski K, Fonfara I, Hauer M, Doudna JA, Charpentier E. A programmable dual-RNA-guided DNA endonuclease in adaptive bacterial immunity. Science. 2012 Aug

17;337(6096):816-21. doi: 10.1126/science.1225829. Epub 2012 Jun 28. PMID: 22745249; PMCID: PMC6286148.

- Kapuscinski J. DAPI: a DNA-specific fluorescent probe. Biotech Histochem. 1995 Sep;70(5):220-33. doi: 10.3109/10520299509108199. PMID: 8580206.

- Karlson CKS, Mohd-Noor SN, Nolte N, Tan BC. CRISPR/dCas9-Based Systems: Mechanisms and Applications in Plant Sciences. Plants (Basel). 2021 Sep 29;10(10):2055. doi: 10.3390/plants10102055. PMID: 34685863; PMCID: PMC8540305.

- Khmelinskii A, Meurer M, Ho CT, Besenbeck B, Füller J, Lemberg MK, Bukau B, Mogk A, Knop M. Incomplete proteasomal degradation of green fluorescent proteins in the context of tandem fluorescent protein timers. Mol Biol Cell. 2016 Jan 15;27(2):360-70. doi: 10.1091/mbc.E15-07-0525. Epub 2015 Nov 25. PMID: 26609072; PMCID: PMC4713137.

- Khosrow-Khavar F, Fang NN, Ng AH, Winget JM, Comyn SA, Mayor T. The yeast ubr1 ubiquitin ligase participates in a prominent pathway that targets cytosolic thermosensitive mutants for degradation. G3 (Bethesda). 2012 May;2(5):619-28. doi: 10.1534/g3.111.001933. Epub 2012 May 1. PMID: 22670231; PMCID: PMC3362944.

- Komander, D., Rape, M. (2012). The ubiquitin code. Annual Review of Biochemistry, 81, 203–229.

- Kondratov, R. V., Kondratova, A. A., Lee, C., Gorbacheva, V. Y., Chernov, M. V., Antoch, M. P., & Gudkov, A. V. (2006). Post-translational regulation of circadian transcriptional CLOCK(NPAS2)/BMAL1 complex by CRYPTOCHROMES. Cell Cycle, 5(8), 890-895.

- Korepanova A, Douglas C, Leyngold I, Logan TM. N-terminal extension changes the folding mechanism of the FK506-binding protein. Protein Sci. 2001 Sep;10(9):1905-10. doi: 10.1110/ps.14801. PMID: 11514681; PMCID: PMC2253207.

- Kuo HP, Hung MC. Arrest-defective-1 protein (ARD1): tumor suppressor or oncoprotein? Am J Transl Res. 2010 Jan 1;2(1):56-64. PMID: 20182582; PMCID: PMC2826822.

- Kuo J, Yuan R, Sánchez C, Paulsson J, Silver PA. Toward a translationally independent RNA-based synthetic oscillator using deactivated CRISPR-Cas. Nucleic Acids Res. 2020 Aug 20;48(14):8165-8177. doi: 10.1093/nar/gkaa557. PMID: 32609820; PMCID: PMC7430638.

- Kuo J, Yuan R, Sánchez C, Paulsson J, Silver PA. Toward a translationally independent RNA-based synthetic oscillator using deactivated CRISPR-Cas. Nucleic Acids Res. 2020 Aug 20;48(14):8165-8177. doi: 10.1093/nar/gkaa557. PMID: 32609820; PMCID: PMC7430638.

- Kuo J, Yuan R, Sánchez C, Paulsson J, Silver PA. Toward a translationally independent RNA-based synthetic oscillator using deactivated CRISPR-Cas. Nucleic Acids Res. 2020 Aug 20;48(14):8165-8177. doi: 10.1093/nar/gkaa557. PMID: 32609820; PMCID: PMC7430638.

- Laptenko, Oleg et al. “The p53 C Terminus Controls Site-Specific DNA Binding and Promotes Structural Changes within the Central DNA Binding Domain.” Molecular and Cellular Biology, vol. 31, no. 8, 2011, pp. 1739-1752.

- Lei, Y., Huang, Y., Lin, J. *et al.* Mxi1 participates in the progression of lung cancer via the microRNA-300/KLF9/GADD34 Axis. *Cell Death Dis* **13**, 425 (2022). https://doi.org/10.1038/s41419-022-04778-w

- Li Z, Rinas U. Recombinant protein production associated growth inhibition results mainly from transcription and not from translation. Microb Cell Fact. 2020 Apr 6;19(1):83. doi: 10.1186/s12934-020-01343-y. PMID: 32252765; PMCID: PMC7137236.

- Naumann C, Mot AC, Dissmeyer N. Generation of Artificial N-end Rule Substrate Proteins In Vivo and In Vitro. Methods Mol Biol. 2016;1450:55-83. doi: 10.1007/978-1-4939-3759-2_6. PMID: 27424746.
- Neklesa TK, Winkler JD, Crews CM. Targeted protein degradation by PROTACs. Pharmacol Ther. 2017 Jun;174:138-144. doi: 10.1016/j.pharmthera.2017.02.027. Epub 2017 Feb 14. PMID: 28223226.
- Nguyen KT, Lee CS, Mun SH, Truong NT, Park SK, Hwang CS. N-terminal acetylation and the N-end rule pathway control degradation of the lipid droplet protein PLIN2. J Biol Chem. 2019 Jan 4;294(1):379-388. doi: 10.1074/jbc.RA118.005556. Epub 2018 Nov 13. PMID: 30425097; PMCID: PMC6322874.

- Nguyen, K.T., Mun, SH., Lee, CS. et al. Control of protein degradation by N-terminal acetylation and the N-end rule pathway. Exp Mol Med 50, 1–8 (2018). https://doi.org/10.1038/s12276-018-0097-y

- Ole K Tørresen, Bastiaan Star, Pablo Mier, Miguel A Andrade-Navarro, Alex Bateman, Patryk Jarnot, Aleksandra Gruca, Marcin Grynberg, Andrey V Kajava, Vasilis J Promponas, Maria Anisimova, Kjetill S Jakobsen, Dirk Linke, Tandem repeats lead to

sequence assembly errors and impose multi-level challenges for genome and protein databases, Nucleic Acids Research, Volume 47, Issue 21, 02 December 2019, Pages 10994–11006, https://doi.org/10.1093/nar/gkz841

- Omachi K, Miner JH. Comparative analysis of dCas9-VP64 variants and multiplexed guide RNAs mediating CRISPR activation. PLoS One. 2022 Jun 28;17(6):e0270008. doi: 10.1371/journal.pone.0270008. PMID: 35763517; PMCID: PMC9239446.

- Partch, C. L., et al. (2014). Molecular architecture of the mammalian circadian clock. Trends in Cell Biology, 24(2), 90-99.
- Peters, J. M., Franke, W. W. (2012). Proteasomes: Protein degradation machines of the cell. Trends in Biochemical Sciences, 37(12), 633–640.
- Pickart, Cecile M., and Robert E. Cohen. "Proteasomes and their kin: proteases in the machine age." Nature Reviews Molecular Cell Biology, vol. 5, no. 3, 2004, pp. 177-187.

- Polevoda B, Brown S, Cardillo TS, Rigby S, Sherman F. Yeast N(alpha)-terminal acetyltransferases are associated with ribosomes. J Cell Biochem. 2008 Feb 1;103(2):492-508. doi: 10.1002/jcb.21418. PMID: 17541948.

- Polevoda, B., & Sherman, F. (2001). N-terminal acetyltransferases and sequence requirements for N-terminal acetylation of eukaryotic proteins. Journal of Molecular Biology, 31(3), 1005-1016.

- Ponugoti B, Kim DH, Xiao Z, Smith Z, Miao J, Zang M, Wu SY, Chiang CM, Veenstra TD, Kemper JK. SIRT1 deacetylates and inhibits SREBP-1C activity in regulation of

hepatic lipid metabolism. J Biol Chem. 2010 Oct 29;285(44):33959-70. doi: 10.1074/jbc.M110.122978. Epub 2010 Sep 3. PMID: 20817729; PMCID: PMC2962496.

- Samarasinghe KTG, Jaime-Figueroa S, Burgess M, Nalawansha DA, Dai K, Hu Z, Bebenek A, Holley SA, Crews CM. Targeted degradation of transcription factors by TRAFTACs: TRAnscription Factor TArgeting Chimeras. Cell Chem Biol. 2021 May 20;28(5):648-661.e5. doi: 10.1016/j.chembiol.2021.03.011. Epub 2021 Apr 8. PMID: 33836141; PMCID: PMC8524358.

- Schneider-Poetsch, T., Ju, J., Eyler, D. et al. Inhibition of eukaryotic translation elongation by cycloheximide and lactimidomycin. Nat Chem Biol 6, 209–217 (2010). https://doi.org/10.1038/nchembio.304

- Senturk S, Shirole NH, Nowak DG, Corbo V, Pal D, Vaughan A, Tuveson DA, Trotman LC, Kinney JB, Sordella R. Rapid and tunable method to temporally control gene editing based on conditional Cas9 stabilization. Nat Commun. 2017 Feb 22;8:14370. doi: 10.1038/ncomms14370. PMID: 28224990; PMCID: PMC5322564.

- Shin HY, Wang C, Lee HK, Yoo KH, Zeng X, Kuhns T, Yang CM, Mohr T, Liu C, Hennighausen L. CRISPR/Cas9 targeting events cause complex deletions and insertions at 17 sites in the mouse genome. Nat Commun. 2017 May 31;8:15464. doi: 10.1038/ncomms15464. PMID: 28561021; PMCID: PMC5460021.

- Sreekanth V, Zhou Q, Kokkonda P, Bermudez-Cabrera HC, Lim D, Law BK, Holmes BR, Chaudhary SK, Pergu R, Leger BS, Walker JA, Gifford DK, Sherwood RI, Choudhary A. Chemogenetic System Demonstrates That Cas9 Longevity Impacts Genome Editing

Outcomes. ACS Cent Sci. 2020 Dec 23;6(12):2228-2237. doi: 10.1021/acscentsci.0c00129. Epub 2020 Nov 18. PMID: 33376784; PMCID: PMC7760466.

- Starheim, K.K., Gromyko, D., Velde, R. et al. Composition and biological significance of the human Nα-terminal acetyltransferases. BMC Proc 3 (Suppl 6), S3 (2009). https://doi.org/10.1186/1753-6561-3-S6-S3

- Sunbin Deng, Ronen Marmorstein, Protein N-Terminal Acetylation: Structural Basis, Mechanism, Versatility, and Regulation, Trends in Biochemical Sciences, Volume 46, Issue 1, 2021, Pages 15-27, ISSN 0968-0004, https://doi.org/10.1016/j.tibs.2020.08.005.

- Swanson, Robert, et al. "A conserved ubiquitin ligase of the nuclear envelope/endoplasmic reticulum that functions in both ER-associated and Matalpha2 repressor degradation." Genes & Development, vol. 15, no. 20, 2001, pp. 2660-2674.

- Synthetic Control of Protein Degradation during Cell Proliferation and Developmental Processes, Jonathan Trauth, Johannes Scheffer, Sophia Hasenjäger, and Christof Taxis, ACS Omega 2019 4 (2), 2766-2778, DOI: 10.1021/acsomega.8b03011

- Takahashi JS, Hong HK, Ko CH, McDearmon EL. The genetics of mammalian circadian order and disorder: implications for physiology and disease. Nat Rev Genet. 2008 Oct;9(10):764-75. doi: 10.1038/nrg2430. PMID: 18802415; PMCID: PMC3758473.

- Tanaka K. The proteasome: from basic mechanisms to emerging roles. Keio J Med. 2013;62(1):1-12. doi: 10.2302/kjm.2012-0006-re. PMID: 23563787.

- Tasaki, T., Sriram, S. M., Park, K. S., & Kwon, Y. T. (2012). The N-end rule pathway. Annual Review of Biochemistry, 81, 261-289.
- Van Damme P, Hole K, Gevaert K, Arnesen T. N-terminal acetylome analysis reveals the specificity of Naa50 (Nat5) and suggests a kinetic competition between N-terminal acetyltransferases and methionine aminopeptidases. Proteomics. 2015 Jul;15(14):2436-46. doi: 10.1002/pmic.201400575. Epub 2015 Jun 5. PMID: 25886145.
- Van Damme, Petra, et al. "N-terminal acetylome analyses and functional insights of the N-terminal acetyltransferase NatB." Proceedings of the National Academy of Sciences, vol. 109, no. 31, 2012, pp. 12449-12454.
- Varshavsky, A. (1991). Naming a targeting signal. Cell, 64(1), 13-15.
- Varshavsky, Alexander. "The N-end rule pathway and regulation by proteolysis." Proceedings of the National Academy of Sciences of the United States of America, vol. 93, no. 8, 1996, pp. 3219-3222.
- Voges, Dietrich, et al. "Ubiquitin-proteasome system." European Journal of Biochemistry, vol. 268, no. 19, 1999, pp. 6065-6083.
- Vousden, K. H., & Prives, C. (2009). Blinded by the Light: The Growing Complexity of p53. Cell, 137(3), 413-431.
- Zhuo, Chenya et al. "Spatiotemporal control of CRISPR/Cas9 gene editing." Nature Communications, vol. 8, no. 1, 2017, p. 2102.